nature human behaviour

Article

https://doi.org/10.1038/s41562-025-02356-6

Multidisciplinary analyses and ancient DNA reveal social inequality and mobility in the Central Plains during the Eastern Zhou period in China

Received: 23 January 2025

Accepted: 13 October 2025

Published online: 30 December 2025

Check for updates

A list of authors and their affiliations appears at the end of the paper

The Eastern Zhou period (771–221 BC), characterized by social stratification, was marked by important inequality. Here the authors analyse 32 skeletons from Songzhuang Cemetery in Henan Province using sex-specific peptides, ancient DNA and isotopes to explore multidimensional inequality in sexes, diet and mobility. DNA and proteomic analyses show that young women were marginalized as sacrificial victims (22 out of 26 human sacrifices were female). Carbon and nitrogen isotopic analyses suggest dietary differences by social class, with the nobility consuming more high-protein and millet-based diets than sacrificial companions, who themselves show intra-group dietary variation ($\delta^{13}C_{bone,nobles} = -8.6‰$; $\delta^{13}C_{bone,human\ sacrifice\ group\ one} = -10.9‰$; $\delta^{13}C_{bone,human\ sacrifice\ group\ two} = -14.1‰$; $\delta^{15}N_{bone,nobles} = 11.6‰$; $\delta^{15}N_{bone,human\ sacrifice\ group\ one} = 8.5‰$; $\delta^{15}N_{bone,human\ sacrifice\ group\ two} = 7.7‰$). Enamel and dentin isotope data indicate that these dietary inequalities were established from childhood ($\delta^{13}C_{enamel,nobles} = -1.5‰$; $\delta^{13}C_{enamel,human\ sacrifice\ group\ one} = -3.8‰$; $\delta^{13}C_{enamel,human\ sacrifice\ group\ two} = -6.9‰$). Strontium and oxygen isotope evidence shows that a high proportion of the nobles were non-local migrants. Genetic analysis reveals a genealogy linking four noblewomen to a sacrificial victim, highlighting the importance of kinship and marital alliances in maintaining social status. Despite class rigidity, dental isotope sequences in M18 reveal that two individuals experienced childhood dietary shifts, indicating rare class mobility.

Understanding and revealing social inequality has long been a central focus in archaeology. Scholars have engaged in extensive and in-depth discussions on various aspects of this topic, including the origins of social inequality, particularly the roles of agriculture and climate[1–3], its manifestations, such as through high-status items, diet, mobility and health[4,5], and the perspectives from which it is observed, including race, gender, age and social class[6]. Additionally, researchers have explored how patterns of social inequality are perpetuated[7,8]. Archaeological findings have facilitated cross-disciplinary connections, thereby validating and refining these models on a global scale. This includes studies on resource inequality, as evidenced by tomb and household scales[9–11], alongside nutrition- and health-related disparities revealed through human bone isotopes[12,13]. Furthermore, ancient DNA provides critical insights into social inequality[14,15], illuminating kinship networks that potentially link specific familial relationships to wealth inheritance[16,17] and sex-biased population dynamics. A classic example is the male-biased Yamnaya expansions, evidenced by disparities in uniparental markers (Y chromosome and mitochondrial DNA) and potential signals in X chromosomes[18–20]. However, variations in natural environments, subsistence methods, resource types, levels

e-mail: 253466072@qq.com; chuanchaowang@fudan.edu.cn; wenshaoqing@fudan.edu.cn; anchuan@ustc.edu.cn

of social development and cultural contexts lead to differing patterns of social inequality across societies. Consequently, systematic research on social inequality in specific periods and regions remains essential globally.

The Eastern Zhou period (770–221 BC) in China marked a significant era of increasing social inequality and institutionalization, laying the groundwork for enduring class and gender disparities in China and East Asia. As the first historical period with extensive documentation, it provides clear evidence of societal hierarchy within its estimated population of tens of millions[21–23]. The ranked segments of the population included the *zhoutianzi* (Zhou king), *zhuhou* (vassals), *qingdafu* (high officials) and *shi* (scholar gentry), alongside commoners and other lower-class individuals who held subordinate positions[24–26]. Archaeological findings, such as variations in tomb sizes, the number of funerary objects (notably the *lieding* (ding sets)) and sacrificial burials, further corroborate this social stratification[27,28].

Despite this, the nobles garnered more literary attention, resulting in a skewed understanding of social stratification. Scholars acknowledge that burial customs not only reflect the social status of individuals during their lifetimes but also represent efforts by the living to portray and reconstruct social realities[29–31]. Consequently, being superior in life is as crucial as being superior in death—the reconstruction of individuals' lifestyles before their death using bioarchaeological methods has been considered for the study of social inequality. The link between diet and social inequality is a major focus, given global hierarchical disparities in the human diet[32–35]. Stable isotopic ratios of $\delta^{13}C$ and $\delta^{15}N$ in bone and tooth collagen reveal distinct dietary patterns, and significant studies have been conducted on the Eastern Zhou population. These studies reveal dietary differences among various ranks at different sites in the Central Plains and Shandong regions. The higher ranks primarily had a millet-based diet and consumed significantly more animal protein, whereas the lower ranks consumed less animal protein and some wheat—a less preferred staple at the time[36–40]. Zhou et al.[39] compared the pre-death diets of nobles, human sacrifices, urban commoners and rural commoners across representative Central Plains sites. The results showed that nobles took millet as their staple food and consumed large amounts of animal protein; in contrast, sacrificial attendants and urban commoners had similar dietary characteristics, eating less millet and less animal protein than nobles, and there was a certain degree of stratification. Rural residents still took millet as their staple food and did not show significant internal differences. This study emphasizes the necessity of studying dietary differences in the context of a broader range of population identities. Dong et al.[41] identified a marked difference in dietary patterns between adult males and females of the Eastern Zhou through isotopic analysis of bone collagen. Further stable isotope analysis of incremental dentin segments traced these differences back to early childhood, suggesting a process of institutionalized gender differentiation during the Eastern Zhou period[42,43].

Social inequality is a multifaceted issue, evident in politics, economics and society, affecting not only resource acquisition and accumulation but also decision-making autonomy[17,44]. Previous research has predominantly examined dietary differences among individuals before death, thereby limiting our understanding of social inequality during the Eastern Zhou. This highlights the need for a more comprehensive approach that considers multiple dimensions of social stratification to fully grasp the patterns of inequality during this era. A particularly suitable site for such a study is Songzhuang Cemetery, located in the eastern part of Songzhuang Village, Qixian County, Hebi City, Henan Province, where 17 tombs from the Eastern Zhou period were excavated (Fig. 1). The tombs illustrate a tripartite social hierarchy—nobles, commoners and sacrificial individuals—through distinct burial practices (Fig. 1)[45]. Nobles were laid to rest in the central coffin chamber, surrounded by inner and outer coffins and accompanied by prestigious items such as bronze tripods, chime bells and jade artefacts, which underscored their elite status. Sacrificial individuals were interred around the noble's coffin chamber; some were placed on a second-tier platform with simple wooden coffins and minimal grave goods, whereas others were located in waist pits without coffins. Commoners, in contrast, had separate burials, typically in wooden coffins with a few pottery items. Carbon and nitrogen stable isotope analysis of the nobles and human sacrifices has revealed dietary variations among social classes, providing a solid foundation for further analysis[40].

In this study, we present proteomic sex identification and ancient DNA analyses, alongside $^{87}Sr/^{86}Sr$, $\delta^{18}O$ and $\delta^{13}C$ data from tooth enamel and $\delta^{13}C$ and $\delta^{15}N$ data from dentin collagen for 32 individuals from Songzhuang Cemetery. The aim of our DNA analyses was to uncover genetic structure differences among social strata and potential kinship among individuals. The focus of our strontium and oxygen isotope analyses was to identify first-generation non-locals. The $^{87}Sr/^{86}Sr$ ratios in human tooth enamel reflect the geological conditions of the area where food was sourced during early tooth formation[46], whereas $\delta^{18}O$ values relate to temperature, elevation and distance from the sea[47]. $\delta^{13}C_{enamel}$, $\delta^{13}C_{dent}$ and $\delta^{15}N_{dent}$ values were used to investigate individual diets during childhood and youth, assessing whether dietary differences among social strata originated in childhood, as previously observed between sexes[43]. Additionally, we considered the stability of individual food intake, given the frequent wars during the Eastern Zhou. Our objective was to elucidate the complex relationships between social stratification and its related dimensions, such as sex, diet, marriage, kinship and mobility, to establish the pattern of social inequality among individuals buried at Songzhuang Cemetery and explore how this pattern was maintained.

Results

Radiocarbon dating

Five new ultrafiltered radiocarbon determinations were obtained from the Songzhuang human skeletal remains, ranging from 2,495 ± 105 (M4) to 2,350 ± 45 ^{14}C years BP (M8) (Supplementary Table 1). This is consistent with the chronological framework of the late Spring and Autumn period to the early Warring States period provided by the archaeological context[45].

Sex determination

Uncertainties in biological sex estimation using traditional osteological methods can often be resolved through the use of genomic and proteomic analyses. In this study, we determined the biological sex of 32 individuals by combining DNA analysis, amelogenin peptide analysis and published physical anthropology results[40]. Among these individuals, five were nobles (comprising four females and one male) and one commoner was identified as female. The group of sacrificial humans exhibited a notably skewed sex distribution, with an exceptionally high proportion of females (22 out of 26). For further details, refer to Supplementary Tables 2–4.

$\delta^{13}C_{enamel}$ values and dentin sequence isotope evidence for childhood diet

We present $\delta^{13}C_{enamel}$ values from 49 tooth enamel samples taken from 31 human individuals, ranging from −0.38 to −9.24‰, with an average of −3.76 ± 2.38‰ (1 s.d.; $n = 49$) (Fig. 2 and Supplementary Table 3). Additionally, isotope analysis of the dentin sequence was conducted on five individuals (Fig. 3 and Supplementary Table 5). The $\delta^{13}C_{dentin}$ values varied from −17.5 to −8.3‰, whereas $\delta^{15}N_{dentin}$ values ranged from 6.8 to 13.8‰. Among the noble individuals, $\delta^{13}C_{dentin}$ values ranged from −15.3 to −8.7‰ and $\delta^{15}N_{dentin}$ ranged from 8.4 to 10.5‰. In contrast, two sacrificial human companions exhibited $\delta^{13}C_{dentin}$ values ranging from −17.2 to −8.3‰ and $\delta^{15}N_{dentin}$ values ranging from 7.5 to 13.8‰. Meanwhile, two sacrificial human offerings showed $\delta^{13}C_{dentin}$ values of −17.5 to −10.8‰ and $\delta^{15}N_{dentin}$ values of 6.7 to 12.1‰.

https://doi.org/10.1038/s41562-025-02356-6

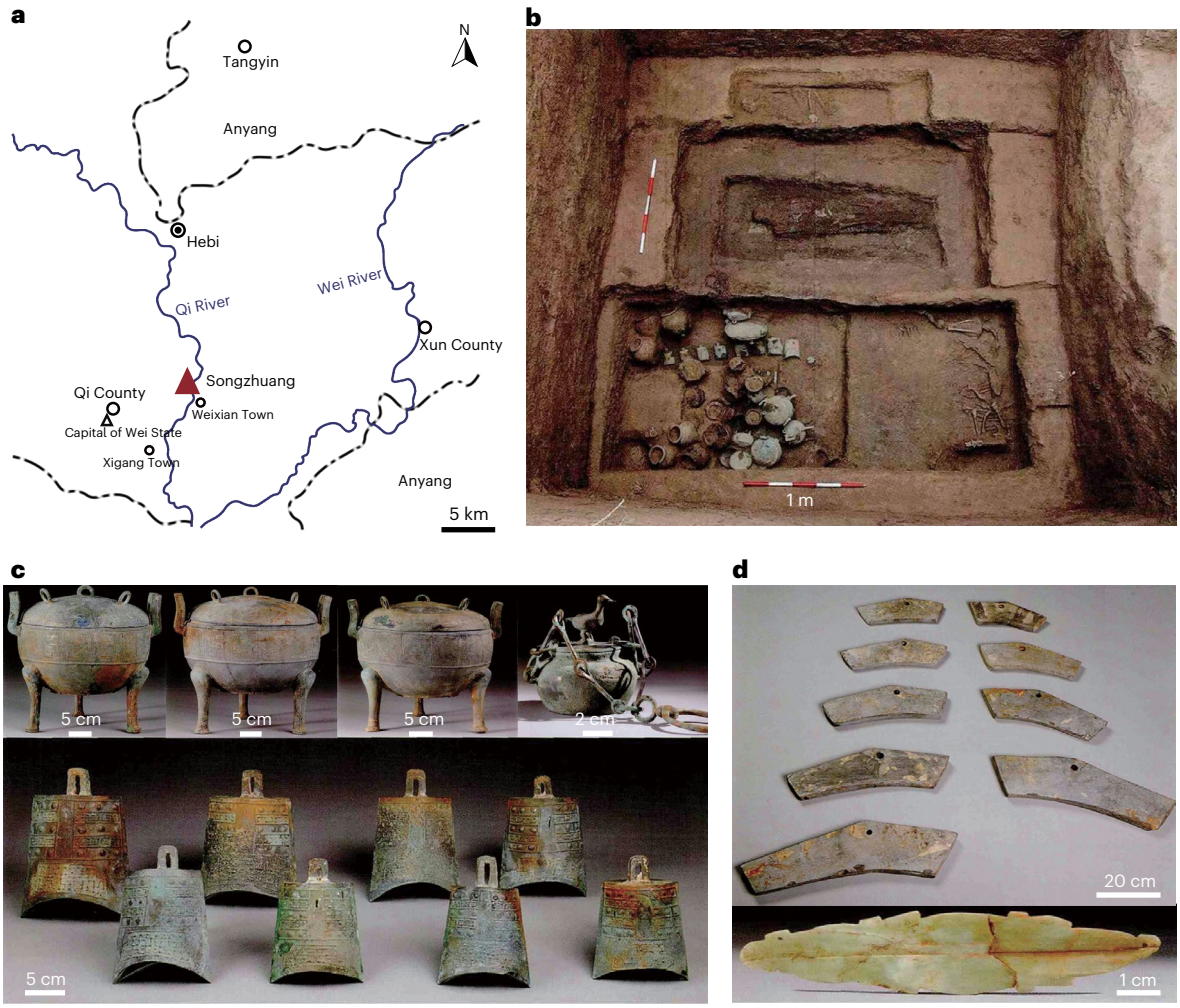

Fig. 1 | Archaeological background of Songzhuang Cemetery. a, Location of Songzhuang Cemetery. **b**, Burial M4 at Songzhuang Cemetery. **c**, Bronze *dings*, a chain-linked pot with standing-bird-shaped lid and a set of bronze chime bells. **d**, A set of stone chimes and jade fish ornaments. Photos in **b**–**d** reproduced from ref. 45.

Dietary variations across social strata. The $\delta^{13}C_{enamel}$ values suggest that all individuals, except M18, predominantly consumed a C_4 diet, assuming an isotopic enrichment from diet to apatite of 12‰ (ref. 48). The $\delta^{13}C_{enamel}$ value of tomb owner M18 was −6.19‰, suggesting the intake of a certain volume of C_3 foods. Among the human sacrifices, dietary patterns varied: some primarily consumed a C_4 diet, whereas others had a mixed C_3/C_4 diet during childhood. To explore potential intra-group dietary differences among the human sacrifices, we divided them into two groups based on burial location, utensils and forms. Group one individuals were not located in waist pits, had wooden coffins and a minority were accompanied by burial objects. Most group two individuals were in waist pits and lacked burial objects. Two special individuals near the outer coffin chamber were assigned to group two due to the presence of violent binding marks on their skeletons (Supplementary Table 3). Figure 2 presents box plots of bone collagen carbon, nitrogen isotopes[40] and tooth enamel carbon isotopes for the nobles, human sacrifice group one and human sacrifice group two. The mean bone collagen carbon isotope values for the three groups were −8.6‰ (n = 2), −10.9‰ (n = 20) and −14.1‰ (n = 4), respectively. The mean bone collagen nitrogen isotope values were 11.6‰ (n = 2), 8.5‰ (n = 20) and 7.7‰ (n = 4), respectively. The mean tooth enamel carbon isotope values were −1.5‰ (n = 8), −3.8‰ (n = 31) and −6.9‰ (n = 6), respectively. Significant differences in carbon isotope values of bone collagen and dental enamel were observed among the differently ranked groups (for bone collagen, $t(22) = 3.543$, $P = 0.002$, Cohen's $d = 1.51$ and 95% confidence interval (CI) = (1.34, 5.10) (two tailed); for dental enamel, $H(2) = 14.275$, $P < 0.001$ and $\varepsilon^2 = 0.30$ (two tailed); Supplementary Tables 6 and 7). The mean difference in nitrogen isotope values of bone collagen between nobles and human sacrifices was relatively large (>3‰), whereas there was an absence of evidence for a significant difference in nitrogen isotope values between the two groups of human sacrifices ($t(22) = 1.658$, $P = 0.112$, Cohen's $d = 0.71$ and 95% CI = (−0.22, 2.01) (two tailed); Supplementary Table 6). Additionally, there was a gradual decrease in both carbon and nitrogen isotope values from the nobles to the human sacrifice group one and further to group two. This suggests that, compared with the former groups, the latter groups consumed more wheat and less meat—a pattern established since childhood.

Nobles exhibit greater dietary stability compared with human sacrifices. The $\delta^{13}C_{enamel}$ values for the nobles were tightly clustered (−0.4‰ to −2.0‰; n = 8), except for M18 (−6.19‰), which may indicate a different childhood identity. In contrast, the carbon isotope values for the human sacrifices displayed a broad range (−1.5 to −9.2‰; n = 36; Fig. 2 and Supplementary Table 3). To capture finer-grained dietary changes, we selected four human sacrifices for isotope analysis of serial dentin sections: two from human sacrifice group one (M1X3 and M18X) and two from human sacrifice group two (M1X5 and M5X4). These four were chosen for distinct $\delta^{13}C_{enamel}$ characteristics: specifically, M1X3, M18X and M1X5 exhibited substantial inter-tooth variations in $\delta^{13}C_{enamel}$

https://doi.org/10.1038/s41562-025-02356-6

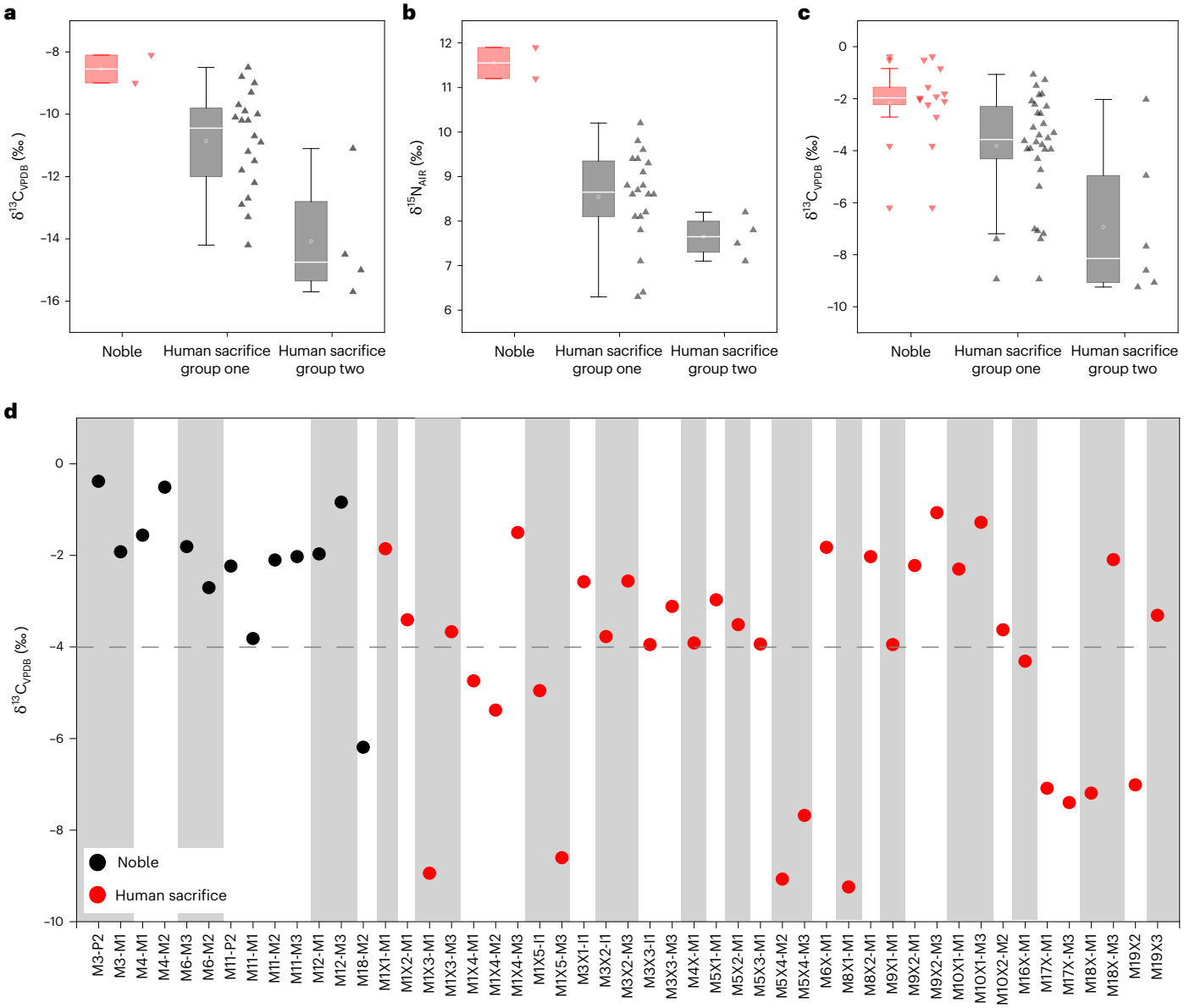

Fig. 2 | Levels of $\delta^{13}C$ and $\delta^{15}N$ in human enamel and bone collagen from individuals buried at Songzhuang Cemetery. a–**c**, Box and scatter plots of phase-based $\delta^{13}C_{VPDB}$ values of human bone collagen (**a**; $n = 2$ (nobles), $n = 20$ (human sacrifice group one) and $n = 4$ (human sacrifice group two)), $\delta^{15}N_{AIR}$ values of human bone collagen (**b**; $n = 2$ (nobles), $n = 20$ (human sacrifice group one) and $n = 4$ (human sacrifice group two)) and $\delta^{13}C_{VPDB}$ values of human enamel (**c**; $n = 13$ (nobles), $n = 30$ (human sacrifice group one) and $n = 6$ (human sacrifice group two)). $\delta^{13}C_{VPDB}$ refers to the ratio of the two stable carbon isotopes ^{13}C and ^{12}C relative to the standard reference material Vienna PeeDee Belemnite, whereas $\delta^{15}N_{AIR}$ refers to the ratio of the two stable nitrogen isotopes ^{15}N and ^{14}N compared with that in Earth's atmosphere. For the box plots, the bounds of the boxes represent 25th and 75th percentiles (defining the interquartile range), the central lines within the boxes represent median values, the whiskers extend to 1.5× the interquartile range from the 25th and 75th percentiles, and the individual data points beyond the whiskers represent statistical outliers in the dataset. Each triangular marker represents the isotopic value of a single bone or tooth enamel sample from a distinct individual. **d**, Scatter plot of enamel $\delta^{13}C$ values showing the isotopic variation between teeth. The *x* axis lists individual IDs along with the tooth analysed (incisor (I), molar (M) or premolar (P)). The grey and white banding identifies separate individuals. The grey dashed line denotes the demarcation between C_4 dietary signals and mixed C_3/C_4 dietary signals. The $\delta^{13}C$ and $\delta^{15}N$ values for bone collagen were obtained from ref. 40.

values (>3‰), whereas M5X4 had unusually low $\delta^{13}C_{enamel}$ values across different tooth positions (Fig. 2d and Supplementary Table 3). Additionally, noble M18 was purposefully selected, given the anomaly in its enamel $\delta^{13}C$ value compared with that of the other nobles. Five individuals could be divided into two groups based on variations in nitrogen isotope values (Fig. 3 and Supplementary Table 5). Group A includes three human sacrifices (M1X3, M1X5 and M5X4), whose nitrogen isotope values remained relatively stable (with a variation range of <2‰), except during the breastfeeding period. For them, the carbon isotope values of the three human sacrifices exhibited substantial intra-dental variances: 8.8‰ (M1X3), 5.8‰ (M1X5) and 6.7‰ (M5X4). This suggests that the consumption of staple foods among the human sacrifices in the Songzhuang Cemetery varied. In general, both the wide range of enamel carbon isotope values across all human sacrifices and the substantial intra-dental carbon isotope variations among group A human sacrifices collectively highlight a greater degree of dietary instability among this population.

Group B comprises a noble (M18) and her associated human sacrifice (M18X). Notable changes in their nitrogen isotope values during their juvenile years suggest a potential shift in social status. For M18,

https://doi.org/10.1038/s41562-025-02356-6

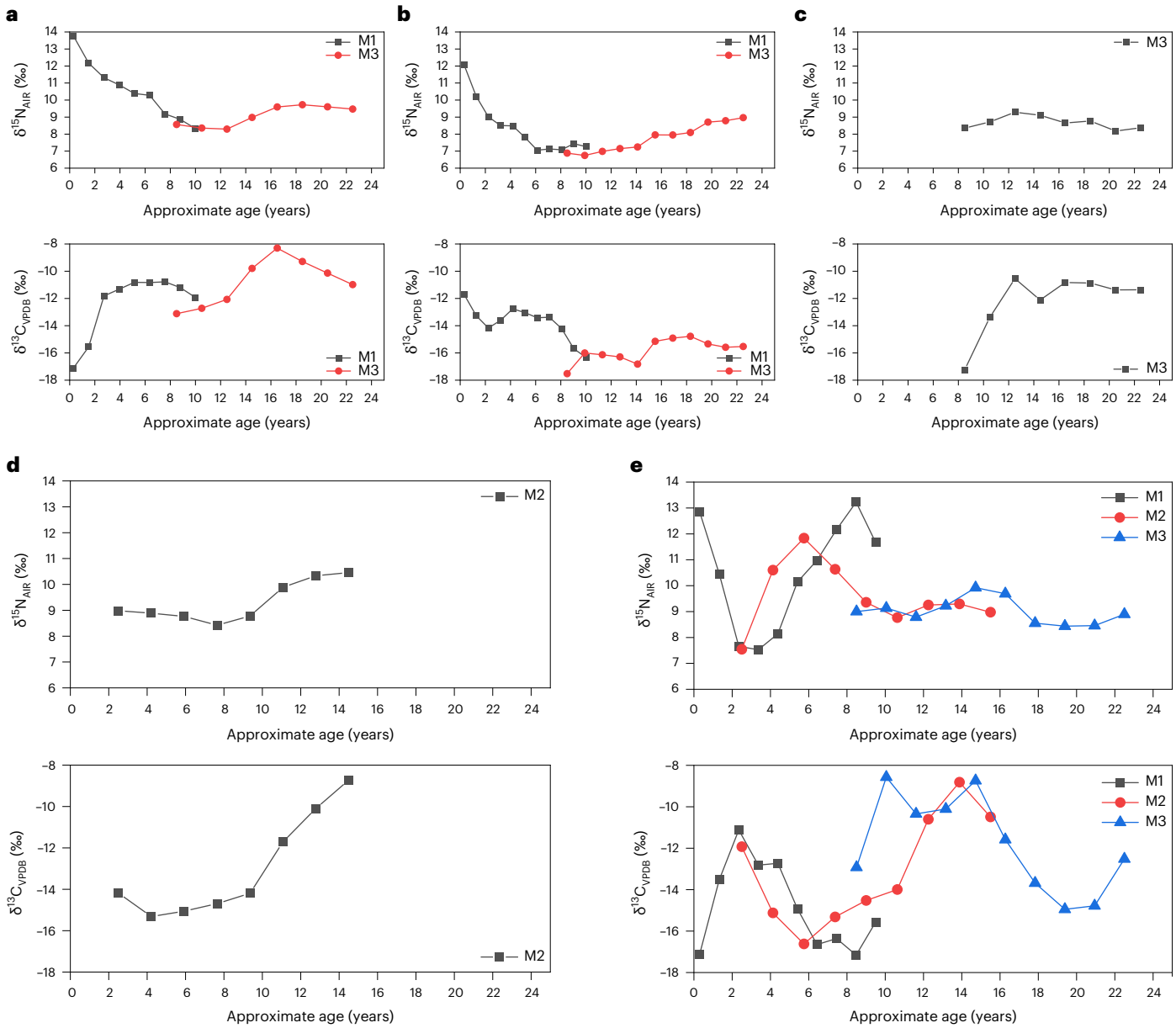

Fig. 3 | Nitrogen and carbon isotopic profiles of dentin serial sections of five humans buried in Songzhuang Cemetery. a–**e**, Values of $\delta^{15}N$ (top) and $\delta^{13}C$ (bottom) for M1X3 (**a**), M1X5 (**b**), M5X4 (**c**), M18 (**d**) and M18X (**e**).

between the ages of 2 and 9–10 years, the $\delta^{13}C_{dent}$ and $\delta^{15}N_{dent}$ values of the second molar remained stable, indicating low meat intake and a mixed C_3/C_4 diet. Between the ages of 10.0 and 14.5 years, the $\delta^{15}N_{dent}$ values increased by 1.5‰, whereas the $\delta^{13}C_{dent}$ values increased by 5.5‰, indicating an increase in protein intake and greater consumption of C_4 foods.

For M18X, between approximately 1 and 4 years of age, the $\delta^{15}N_{dent}$ values decreased consistently by ~5.3‰ (from 12.8 to 8.5‰), suggesting she was probably weaned at 3–4 years of age. After weaning, between 5 and 8 years of age, the $\delta^{15}N_{dent}$ values rose sharply to 13.2‰, whereas the $\delta^{13}C_{dent}$ values decreased to −17.2‰, indicating a further increase in meat intake and consumption of C_3 foods. However, after this period, the situation deteriorated. From age 10 years onward, the $\delta^{15}N_{dent}$ values fell to between 8 and 9‰ and remained at this level until 22–23 years of age, with the $\delta^{13}C_{dent}$ values fluctuating substantially—similar to those of other human sacrifices in the Songzhuang Cemetery.

Strontium and oxygen isotopic evidence of human movement

The results of the strontium isotope analysis for individuals from Songzhuang are summarized in Fig. 4 and Supplementary Table 3. The average $^{87}Sr/^{86}Sr$ value for human tooth enamel samples was 0.711756 ± 0.00043 (1 s.d.), ranging from 0.710470 to 0.713356 (n = 50). Eight local plant and faunal samples were analysed to establish the local strontium isotope range, yielding values between 0.711278 and 0.711726. Additionally, the $^{87}Sr/^{86}Sr$ range for soil and animals in the nearby Xinxiang and Anyang regions was approximately 0.7113–0.7122 (refs. 49,50), providing further confidence in the local $^{87}Sr/^{86}Sr$ range. Nineteen individuals, including four nobles and 15 human sacrifices, showed at least one $^{87}Sr/^{86}Sr$ value outside the local range, suggesting that they spent part of their childhood in different regions. Nonetheless, most of these individuals still aligned with the bioavailable $^{87}Sr/^{86}Sr$ ratio characteristic of the northern part of Henan Province. Exceptions include one noble (M3) and two human sacrifices (M1X1 and M8X2), whose $^{87}Sr/^{86}Sr$ values distinctly fall outside the range of

https://doi.org/10.1038/s41562-025-02356-6

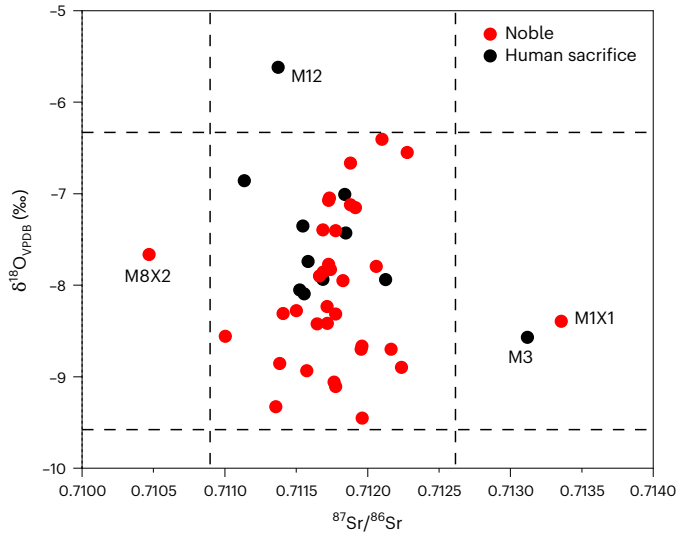

Fig. 4 | Scatter diagram of $^{87}Sr/^{86}Sr$ versus $\delta^{18}O_{VPDB}$ values of human enamel from individuals buried at Songzhuang Cemetery. $\delta^{18}O_{VPDB}$ refers to the ratio of ^{18}O and ^{16}O compared relative to the Vienna PeeDee Belemnite standard. The boundaries formed by the black dashed lines are defined as the local range established based on the isotopic data of the Songzhuang population, calculated as the mean ± 2 s.d. Specifically, the horizontal black dashed lines delineate the reference interval for local $\delta^{18}O_{VPDB}$ values, while the vertical black dashed lines delineate the reference interval for local $^{87}Sr/^{86}Sr$ values.

0.710896–0.712616—defined as the mean ± 2 s.d. of $^{87}Sr/^{86}Sr$ values for the Songzhuang population. Specifically, M8X2 (0.710470) exhibits a value below this range, while M3 (0.713120) and M1X1 (0.713356) have values above it (Fig. 4 and Supplementary Fig. 1).

The $\delta^{18}O$ values of human tooth enamel from Songzhuang ranged from −9.5 to −5.6‰, with a mean of −7.9 ± 0.80‰ (±1 s.d.; $n = 49$). Using two standard deviations from the mean, we define a range of −9.5 to −6.3‰ for individuals who grew up around Songzhuang. The $\delta^{18}O$ value for a civilian (M12) fell outside of this range, indicating that she was non-local (Fig. 4 and Supplementary Table 3).

Integrating the strontium and oxygen isotope results, we infer that at least four individuals buried at the Songzhuang Cemetery originated from beyond the northern part of Henan Province. For individuals with strontium isotope values higher than 0.7130, two regions in the middle and lower reaches of the Yellow River have shown similar isotope ratios. One is the Tai-Yi Mountain range in Shandong Province and its surrounding areas, such as the Dawenkou and Yinjiacheng sites[51,52]; the other is the area around the Qinling Mountains, as indicated by environmental strontium isotope values[53,54]. However, due to the relatively high oxygen isotope values in the Shandong region (for example, the oxygen isotope values of humans at the Yinjiacheng site range from −3.8 to −5.0‰; Supplementary Table 8 and Supplementary Fig. 4), this area was excluded as a potential origin for M3 ($\delta^{18}O$ = −8.5‰) and M1X1 ($\delta^{18}O$ = −8.4‰). Consequently, the Qinling area is considered the possible origin of these two individuals. Furthermore, another piece of evidence is that M3 is the sole tomb owner with a flexed-limb burial in this cemetery, a highly prevalent burial pattern in Qin culture[55]. M12 had the lowest $\delta^{18}O$ value (−5.6‰), which may indicate a childhood in the Shandong coastal area.

Genetic structure and kinship of Songzhuang individuals

We collected ancient DNA data from 24 samples at Songzhuang Cemetery (Supplementary Table 4). All samples exhibited the characteristic patterns of ancient DNA damage, confirming the presence of authentic ancient DNA (Supplementary Fig. 5). To assess the extent of modern human contamination, we utilized mitochondrial-based contamMix for all individuals and X chromosome-based ANGSD software for all male individuals (Supplementary Table 4). We trimmed eight base pairs from each end of the reads and called single-nucleotide polymorphisms (SNPs) at all positions of the 1,240,000-SNP panel. Various kinship inference methods were employed to estimate the relationships between samples, considering the results reliable when at least 10,000 overlapping SNPs were present between samples. Ultimately, we identified four pairs of individuals sharing third-degree kinship (Supplementary Tables 9 and 10): M3–M4, M6–M18, M18–M3X1 and M6–M3 (despite having only 9,772 overlapping SNPs). These five female individuals were grouped into a large family tree (Fig. 5). Interestingly, archaeological evidence inferred that three pairs of third-degree relatives were of noble status, potentially suggesting a connection between social stratification and kinship. We excluded samples with DNA contamination levels exceeding 3%, those with fewer than 20,000 SNPs and those related to other individuals but with lower SNP counts (Supplementary Table 4). Ultimately, we obtained genome-wide data from 24 individuals, covering 49,594–914,277 SNPs for population genetic analysis (Supplementary Table 4). This dataset was merged with published data from modern and ancient individuals.

We analysed the mitochondrial and Y chromosomal haplogroups of individuals from Songzhuang. Among the samples, there were three male individuals, none of whom held noble status. Their Y chromosome haplogroups were identified as O2a2b1a1a (Oα), O2a2b1a2a1a (Oβ) and O2a1b1a1a1a1 (Oγ). These haplogroups represent lineages that experienced rapid expansion during the Late Neolithic period and are widely distributed across China[56]. We successfully identified mitochondrial haplogroups in 21 samples. These included lineages prevalent in both northern and southern East Asia. Haplogroups C, D4, D5, G, N9 and Z were found in 71.4% of the samples (15 out of 21) and are primarily distributed in northern East Asia, whereas haplogroups F, B4 and B5 were present in 28.6% of the samples (six out of 21) and are mainly found in southern East Asia[57]. We conducted principal component analysis (PCA) and admixture analysis to qualitatively assess the genetic affinities of the ancient individuals (Fig. 6). The PCA results displayed a triangular pattern, with modern populations from Northeast Asia, Southeast Asia

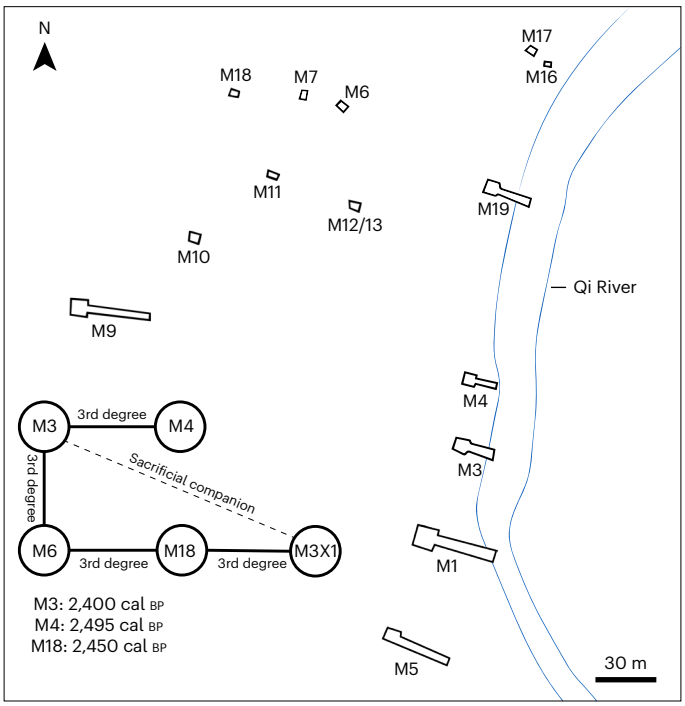

Fig. 5 | Pedigree found in Songzhuang Cemetery and layout of the tombs. The family tree is shown for four pairs of individuals sharing third-degree kinship. cal BP, calibrated years before the present.

https://doi.org/10.1038/s41562-025-02356-6

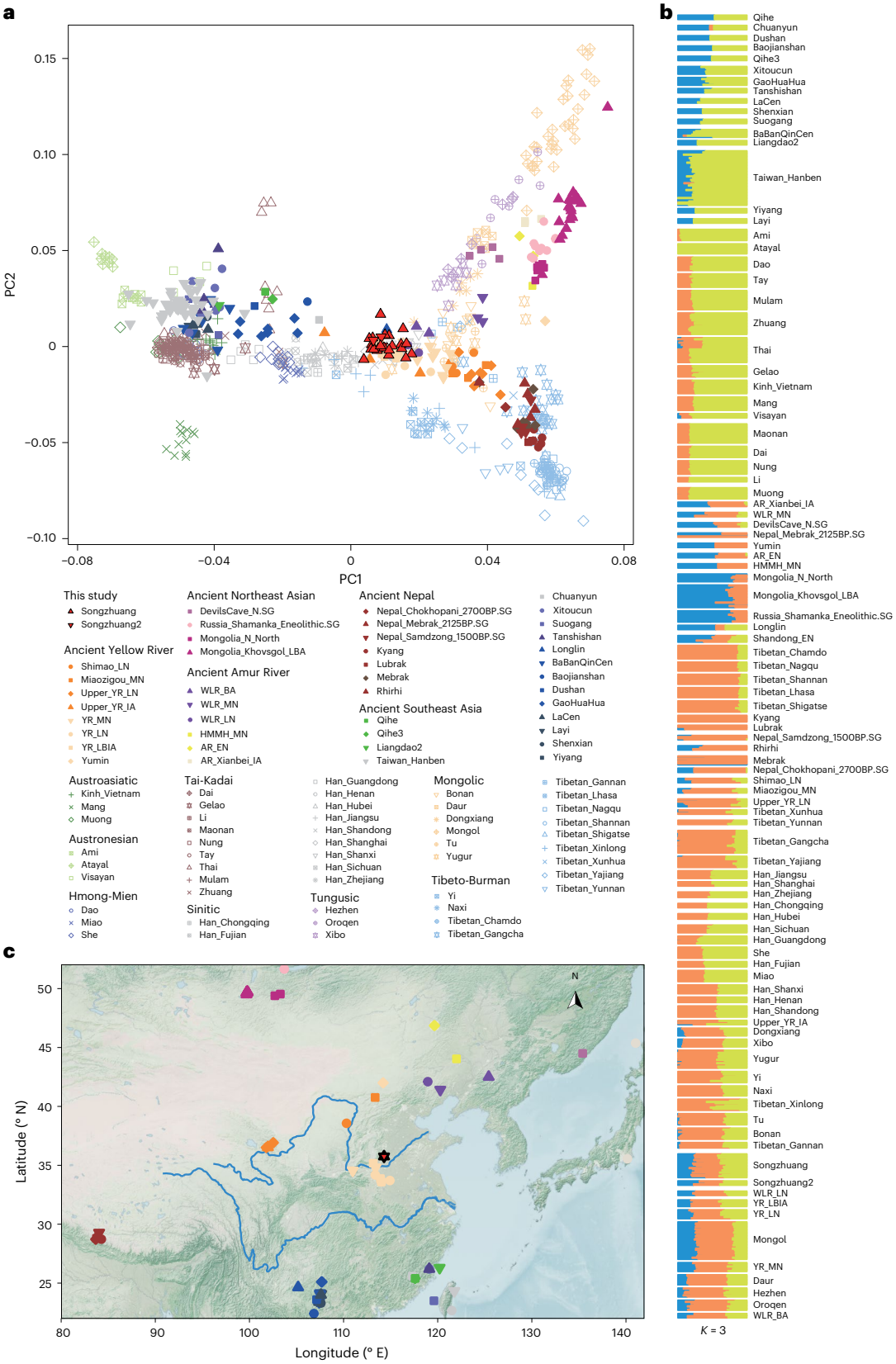

Fig. 6 | PCA and admixture results and geographic locations of ancient individuals. a, PCA plot of ancient and present-day East Asians, incorporating newly sequenced samples from the Songzhuang archaeological site, totalling 24 individuals, with distinct subsets labelled as Songzhuang (21 samples) and Songzhuang2 (three samples). **b**, Admixture analysis results ($k = 3$) of the relevant individuals included in the PCA. The genetic components for highland Tibetan-related populations and those of the upper reaches of the Yellow River are represented by orange, those of southern East Asians are shown in yellow and those of northern East Asians are shown in blue. **c**, Geographic locations of ancient individuals in East Asia, plotted using the NASA Explorer Base Map from Visible Earth (image data by Joshua Stevens/NASA).

and the Tibetan Plateau at the three vertices. The Songzhuang individuals overlapped with ancient populations from the Late Neolithic to the Iron Age Middle Yellow River basin (YR_LN and YR_LBIA, respectively). However, no distinct clustering features were observed in the qualitative analysis. The admixture analysis (Fig. 6) yielded results similar to those of the PCA, revealing high genetic homogeneity among populations near the Central Plains.

Consequently, we performed a further quantitative analysis to investigate the differences between the samples. We performed outgroup f_3 analysis in the format f_3(Songzhuang populations, Reference populations; Mbuti) based on the dataset comprising 1,240,000 SNPs (Fig. 7 and Supplementary Table 11). The Songzhuang samples displayed strong genetic drift shared with Yellow River-related populations, with f_3 values of 0.303–0.315 for Songzhuang samples (Supplementary Table 11). Furthermore, we performed outgroup f_3 analysis in the format f_3(YR_LBIA, Songzhuang; Mbuti) to assess the genetic relationship between Songzhuang samples and those of individuals from the Late Bronze to Iron Age Middle Yellow River (YR_LBIA), who overlapped in location and period (Supplementary Fig. 6 and Supplementary Table 11). We observed slightly lower genetic homogeneity between sample SZ_I52903 (M10X1) and YR_LBIA (f_3 values = 0.305, compared with >0.307 for all other individuals; Supplementary Fig. 6 and Supplementary Table 11). Additionally, qpWave analysis (Supplementary Table 12) confirmed that the Songzhuang samples could be divided into two groups: Songzhuang and Songzhuang2 (with Songzhuang2 comprising SZ_IA0606, SZ_IA2020 and SZ_I52903; see Supplementary Table 4 for individual IDs, feature numbers and group labels). We used f_4 statistics in the format f_4(Mbuti, references; Songzhuang, Songzhuang2) to compare genetic differences between Songzhuang and Songzhuang2 (Fig. 7) and found significant negative values ($Z < -3$) when using Hezhen, Nepal_Samdzong_1500BP, Shimao_LN and Nepal_Chokhopani_2700BP as reference populations. Pairwise qpWave analysis suggested that Songzhuang could be modelled as driving a single wave of ancestry from Late Neolithic to Iron Age Middle Yellow River farming groups (YR_LN and YR_LBIA; Supplementary Table 12), but Songzhuang2 could not ($P < 0.001$) due to an excess affinity with southern East Asians compared with Yellow River farmers (Supplementary Fig. 7). Using Tanshishan as a surrogate for ancient southern East Asians, we modelled Songzhuang2, which derived 18.1% (s.e.: 3.8%; 95% CI: 10.7–25.5%) of its ancestry from Tanshishan and the rest from YR_LBIA ($\chi^2(7) = 9.140$; $P = 0.2427$; Fig. 7 and Supplementary Table 12). This result further confirms that the noble sample SZ_IA0606 (M18), included in Songzhuang2, is more likely to be related to southern China. Overall, intermarriage and interactions between northern and southern elites indicate social connections or alliances among regional elite groups.

Discussion

Pattern of social inequality in Songzhuang society

A multidisciplinary analysis allows for a comprehensive reconstruction of social inequality patterns in Songzhuang Cemetery. Burial practices, including the types of burial objects and structures, reveal significant disparities, embodying the notion of living as though in death. Nobles were interred with coffins, outer coffins and an abundance of funerary objects, including ritual and musical instruments, which served as primary status symbols. In contrast, commoners (for example, M12) were buried with a single coffin and simple pottery. Human sacrifices surrounded the tomb owners, with some placed on a second-tier platform alongside wooden coffins and others in waist pits devoid of burial equipment. Two individuals (M8X1 and M8X2) on the second-tier platform exhibited signs of violent death. Some sacrificial victims had basic burial objects, such as string ornaments, bone hairpins and small jade and bronze items, highlighting differences within the sacrificial group.

The predominance of young females (22 out of 26) in the sacrificial group suggests a potential marginalization of women in Songzhuang society. Archaeologists have identified these young female sacrificial individuals as either female attendants (*shìbì*) or entertainers (*jìyuè*)[58–61], who provided services and entertainment to the nobility and were buried with them upon their deaths. Despite the stark gender imbalance, the most richly buried sacrificial individual was a male, M19X3, who was interred with a bronze belt hook and a jade plaque, further emphasizing the harsh realities faced by lower-class women and the gender disparities of that era.

As previously noted, the development of social inequality had a significant impact on diet, as reflected in Songzhuang society. Nobles primarily consumed a millet-based diet with a higher animal protein intake, whereas lower-status individuals had limited access to animal protein and consumed some wheat. The high meat consumption of the nobility aligns with the meat-eaters status documented in classical texts, such as the *Zuo Zhuan*. In contrast, the divergence in staple grain consumption probably stemmed from varying access to newly introduced wheat cultivars during the Zhou agricultural transition. Long-term archaeobotanical studies indicate that during the Zhou period in the middle and lower Yellow River regions, wheat was widely cultivated and became the second most important crop after foxtail millet at most sites[62–65]. Climate deterioration, technological advancements and population growth may have driven the widespread cultivation of wheat. At the end of the Holocene climatic optimum (approximately 3,000 BP), the climate became progressively cooler and drier[66]. Archaeobotanists have noted a widespread decline of rice, a crop with high hydrothermal demands, in the lower and middle reaches of the Yellow River around 3,000 BP[66]. Meanwhile, historians emphasize the rapid population growth during the Zhou Dynasty, particularly in the Eastern Zhou period[21]. Consequently, under the pressures of climate change and population growth, wheat, as a high-yield dryland crop, became an essential food supplement. However, the introduction of new crops was not equally embraced by all social groups. Isotopic evidence suggests that lower-status individuals consumed more wheat. Simultaneously, as noted by Tian and Zhou[67], historical documents and bronze inscriptions detailing the diets of Zhou Dynasty elites reveal a limited presence of wheat. The primary reason for this differential acceptance probably relates to the food processing methods used. During the initial phase of wheat introduction, it was primarily prepared as whole grains, which did not fully separate the husk from the wheat kernels[68]. This resulted in a coarse texture and poor digestibility. Consequently, for aristocrats not pressured by food scarcity, it is understandable why wheat did not become a staple food for Eastern Zhou elites.

Further analysis provides additional details on dietary differences, including inter-group variations among sacrificial individuals, the establishment of dietary patterns in early life and the instability in the diet of the sacrificial population. The diet of human sacrifices varied within the group, with those in the waist pits and the two individuals on the second-tier platform showing binding marks and having lower dietary levels (lower carbon and nitrogen isotope values) than other individuals. Dental isotope analysis indicates that dietary differences among individuals of different ranks emerged during childhood in the Eastern Zhou. Combined with childhood differences between the sexes[43], this provides institutionalized evidence of class and gender inequality during that period. Additionally, the high variability of carbon isotopes among teeth suggests significant changes in the staple foods of the human sacrifice group throughout their lives, possibly reflecting their limited ability to withstand risks. In times of food shortages due to famines, wars and other factors, human sacrifices may have been forced to consume less desirable foods such as wheat, whereas nobles maintained an ideal diet. It is important to highlight the temporal and spatial limitations of these conclusions. Specifically, any assertions about disparities in wheat consumption should be confined to the Eastern Zhou period. This is because climate change, agricultural restructuring and advancements in crop processing techniques

https://doi.org/10.1038/s41562-025-02356-6

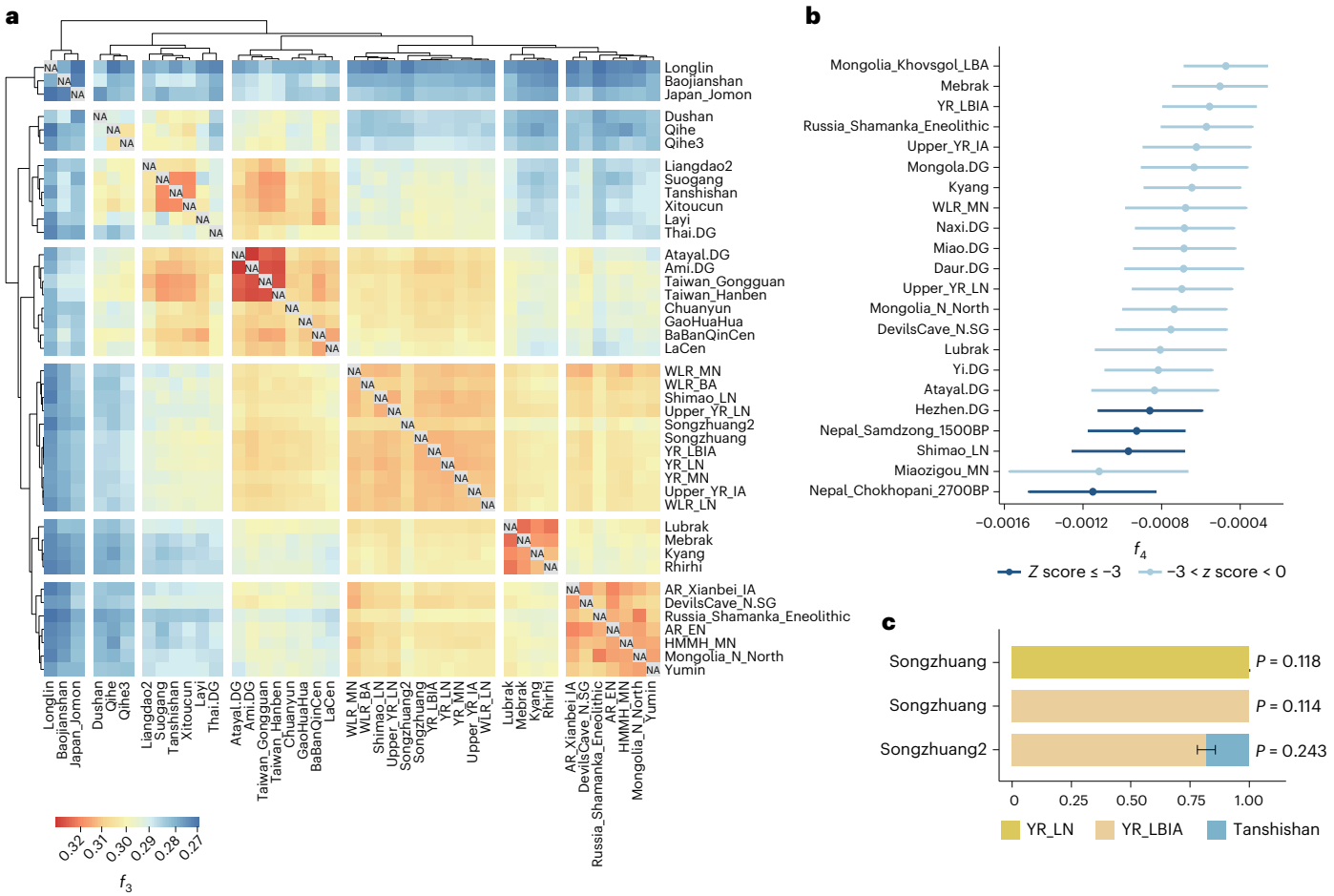

Fig. 7 | Quantitative analysis results. a, Heatmap of outgroup f_3 statistics in the format f_3(ancient samples, ancient samples; Mbuti). 'NA' denotes intra-population comparisons (for example, popA versus popA), which were excluded as they could not provide meaningful signals of genetic affinity. **b**, Results of f_4 statistical analysis in the format f_4(Mbuti, references; Songzhuang, Songzhuang2). **c**, Modelling results for Songzhuang and Songzhuang2 by qpAdm, which applies a Hotelling's T^2 test (two tailed). The error bar represents ±1 s.e. The uncorrected P values serve as a critical metric for model selection, aiming to identify a single, well-fitting historical hypothesis ($P > 0.05$). Multiplicity correction is inappropriate in this context.

would have influenced dietary patterns over time. Additionally, due to the limited sample size of sacrificial victims in this study, further research is needed to explore the intra-group dietary differences of these individuals within a broader site context.

Finally, strontium and oxygen isotope analysis indicates that the tomb occupants had a higher proportion of non-local individuals (two out of six) compared with the human sacrifices (two out of 26), suggesting greater mobility among the tomb occupants.

Compared with other Zhou Dynasty sites, patterns of social inequality appear to vary, with notable differences in sex ratios and dietary patterns. We collected sex information of human sacrifices from 26 Zhou Dynasty sites and dietary information from differently ranked groups at six sites, all from previously published data[37,39,69–87]. The findings reveal that, compared with other regions, the Central Plains and Shandong areas more frequently used females as burial companions, with female human sacrifices exceeding 80% at each site (Supplementary Table 13 and Supplementary Fig. 2). This may indicate unique cultural practices and sacrificial systems in these regions, whereas other areas did not exhibit a clear gender preference in sacrifices. Although only seven sites provided comparable isotope data, significant changes in dietary patterns over time are evident[37,69,74,84–87] (Supplementary Table 14 and Supplementary Fig. 3). During the Western Zhou Dynasty, research on three sites (Hengshui[87], Dahekou[86] and Xinancheng[84]) showed that, although the average $\delta^{13}C$ values of high-status individuals were lower than those of low-status individuals, the difference was minimal (within 1‰), indicating similar staple foods across social statuses. During the Eastern Zhou period, hierarchical dietary differences emerged, with higher $\delta^{13}C$ values observed in individuals of higher social status compared with those of lower social status. Significant differences were noted at three sites in the middle and lower reaches of the Yellow River (SJNT[69], ZHGC[85] and DH[37]; Supplementary Table 15 and Supplementary Fig. 3). These temporal and spatial variations underscore the need to further explore different patterns of social inequality.

Consanguinity and affinity relationships perpetuate social inequality

In Songzhuang society, two female nobles exemplified a potential pattern of female exoticism. As previously noted, multi-isotopic and burial analyses suggest that M3 may have spent her childhood in the Qin cultural area. Meanwhile, ancient DNA results for M18 indicate partial ancestry from southern China, implying origins south of the Yellow River basin, such as the Chu State, or parentage from both the Yellow River basin and southern regions. M18's genetic profile also reflects the outcome of inter-ethnic marriage. Kinship analysis confirmed that four nobles belonged to the same extensive lineage, with ^{14}C dating showing M4 to be approximately 100 years younger than M3, suggesting a possible descendant relationship

(Supplementary Table 1 and Fig. 5). These findings imply that consanguinity and affinity relationships played significant roles in maintaining and transmitting social inequality within Songzhuang society.

The Zhou Dynasty was characterized by a patriarchal lineage system in which consanguinity played a significant role in maintaining societal hierarchies. This study uncovered an aristocratic lineage lasting around one century, underscoring the importance of consanguinity in the inheritance of aristocratic status (Fig. 5). A parallel situation was observed in the Bronze Age in Germany, where a detailed microregional study of 104 individuals over 700 years revealed a society comprising a high-status core family and unrelated low-status individuals—a structure that persisted through generations[17]. Simultaneously, exogamy and political marriages have been significant worldwide for maintaining political alliances[17,88–90]. In China, multivariate isotope analysis of individuals from Xiajin Cemetery in the late Neolithic period suggests a high level of female mobility, interpreted as evidence of exogamy[91]. Historical documents also recount political marriages involving women during the Zhou Dynasty. For example, *The Book of Songs*[92] details the complex connections of Lady Zhuang Jiang, who was "the daughter of the Marquis of Qi, the wife of the Marquis of Wei, the sister of the Crown Prince, the aunt of the Marquis of Xing, and the sister-in-law of the Duke of Tan", thereby linking the five vassal states of Qi, Wei, Lu, Xing and Tan through her familial ties.

Evidence of social class mobility from the tomb of M18

The noble individual M18, an adult female, exhibited a $\delta^{13}C_{enamel}$ value that was not only lower than that of other nobles but also lower than that of most sacrificial individuals (Supplementary Table 3), indicating a significant intake of C_3 foods. Her sacrificial companion showed a similar pattern. For M18X, the $\delta^{13}C_{enamel}$ value of the first molar (M1) was −7.2‰, suggesting substantial consumption of C_3 foods, whereas the third molar (M3) showed a $\delta^{13}C$ value of −2.1‰, reflecting a shift in dietary staples. To better understand the reasons behind this change, we conducted dentin sequence isotope analysis on the teeth of M18 and M18X, revealing completely divergent life courses (Supplementary Table 5 and Fig. 3). As previously analysed, M18 underwent a dietary shift around the age of 10 years, characterized by an increase in both nitrogen isotope values (1.5‰) and carbon isotope values (5.5‰). This dietary pattern shifted from resembling that of low-ranking commoners or human sacrifices of the period to matching that of other noble individuals in Songzhuang Cemetery. For M18X, a contrasting and notable change also occurred around the age of 10 years. After weaning and before the age of 10 years, this individual's $\delta^{15}N_{dent}$ values peaked at 13.2‰, whereas $\delta^{13}C_{dent}$ values decreased to as low as −17.2‰. This isotopic signature suggests a diet akin to that of nobles in the Chu State in southern Henan, such as those in Chengyang City and Xinzhuang[38]. We reasonably conclude that the low carbon isotope values during this stage might be attributed to rice consumption. However, around the age of 10 years onwards, the situation deteriorated: $\delta^{15}N_{dent}$ values fell to between 8 and 9‰ and remained at this level until ages 22–23 years, with $\delta^{13}C_{dent}$ values fluctuating significantly—similar to those of other human sacrifices in Songzhuang Cemetery. Overall, the isotopes appear to indicate M18's transition from a low-status individual to a high-status individual, whereas the opposite was true for M18X. Ancient DNA results show that M18 had additional southern gene flow compared with other individuals in Songzhuang, indicating that both M18 and her sacrificial victims probably lived in the south (south of Songzhuang Cemetery, such as southern Henan) during childhood. They experienced a reversal of status around the age of 10 years, moved to Songzhuang and were ultimately buried there.

During the Eastern Zhou period, society was tumultuous, marked by frequent wars. Social status could be gained through personal efforts or lost due to political or military failures. Historical figures such as Zhang Yi of the Qin State and Shen Buhai of the Han State exemplify status ascension through talent. Classics such as the *Zuo Zhuan* and *Guoyu* also document such instances: "In the twentieth year of Duke Zhao, Wu Yuan (a nobleman of the Chu State) went to the state of Wu… he remained to labor in the wild"[93] and "The Zhonghang and Fan lineages, neglecting the hardships of the common people, sought to seize control of the state of Jin. Now their descendants will till the fields in Qi, and the sacrificial animals of their ancestral temples have become laborers in the fields"[94]. Having lost in political struggles, members of aristocratic families such as those of Wu Yun, Zhonghang and Fan eventually became farmers. The M18 tomb in Songzhuang Cemetery provides compelling bioarchaeological evidence of shifting social statuses during the Eastern Zhou, revealing that in times of social upheaval the pattern of inequality was dynamic and ever changing.

Conclusion

Our study utilized a multidisciplinary approach to uncover the profound impacts of social inequality during the Eastern Zhou period. The marginalization of young women as sacrificial companions and stark differences in diet and mobility between nobles and companions underscore the entrenched class divisions of the time. By reconstructing noble family networks, we demonstrate the importance of kinship and marital alliances in maintaining elite status. Furthermore, evidence of class mobility provides rare insights into social flexibility. This research deepens our understanding of the origins and complexities of ancient social inequality, providing critical perspectives on the dynamics and diversity of early Chinese society. The findings also highlight the potential of multidisciplinary methodologies in uncovering patterns of social inequality in past civilizations.

Despite analysing all individuals excavated from the Songzhuang site and integrating published datasets, our conclusions are inherently limited by the extensive demographic scale and complex social structure of the Eastern Zhou period. Two critical directions are prioritized for future work: (1) enhancing the temporal and spatial resolution of sampling to detect potential regional and chronological variations in patterns of social inequality; and (2) expanding the diversity of social strata analysed, particularly by incorporating commoner populations—an essential demographic currently underrepresented in our dataset, which limits comprehensive interpretations of this complex society. Addressing these gaps will enable more nuanced reconstructions of social inequality during this pivotal era.

Methods

Ethics and permissions

Our sampling and analysis approach for ancient DNA research on human remains followed the guidelines for best practice[95]. All human skeletal remains analysed in this study were sampled with written permission from the Henan Provincial Institute of Cultural Relics and Archaeology. Descriptions of the archaeological and cultural contexts for all ancient samples analysed—including their grave position within archaeological sites, grave numbers and burial inventory, as well as references to archaeological publications for the sites—are provided in the main text and Supplementary Table 3.

Radiocarbon dating

Five human bone collagen samples from different tombs were dated at the accelerator mass spectrometry radiocarbon dating laboratory of the Key Laboratory of Western China's Environmental Systems (Ministry of Education) at Lanzhou University[96]. OxCal version 4.4.4 (ref. 97) with the IntCal20 calibration curve[98] was used to calibrate all of the radiocarbon dates. All reported ages are relative to AD 1950 (referred to as years BP).

Proteomic analysis

Amelogenin, found in dental enamel, is expressed in humans as two isoforms derived from genes located on the non-recombining regions of the X and Y chromosomes. The precise identification of

amelogenin Y-specific sequences provides a robust method for sex determination[99–102]. As the hardest tissue in the human body, dental enamel preserves amelogenin exceptionally well, allowing for reliable sex determination of human remains under various preservation conditions, including those of ancient ancestors dating back hundreds of thousands of years[103,104]. In this study, we performed proteomic analysis on six individuals (M3, M6, M11, M12, M18 and M10X1) whose biological sex could not be determined through osteological methods.

Protein extraction. We processed the enamel following previously described protocols[105]. The surface of each tooth was scraped with a dental burr to remove visible surface contaminants. Enamel samples were then rinsed with 3% H_2O_2 (10011218; SCR) for 30 s, followed by a wash with ultrapure water. A volume of 60–100 µl 1.5 M HCl (CD433036; Codow) was placed in the cap of a 1.5-ml Eppendorf tube. Etching was conducted by submerging the tooth in the HCl solution and maintaining this contact for 20 min; the resulting etching solution was then gathered into a 1.5-ml Eppendorf tube. Some samples were etched more than once. Desalination and elution procedures followed the method described by Stewart et al.[99]. Finally, 10 µl elution buffer (comprising 60% acetonitrile and 0.1% formic acid) containing peptides was dried via centrifugation in a drying centrifuge. A blank control was included throughout the process to track potential contamination during experimentation.

Nano-liquid chromatography tandem mass spectrometry analysis. Dried peptides were reconstituted in 10 µl of a 0.1% formic acid solution and analysed using an EASY-nLC 1200 nanoflow liquid chromatography system (Thermo Fisher Scientific) connected to a Q Exactive Plus mass spectrometer (Thermo Fisher Scientific). A 1-µl aliquot of each sample was injected onto a pre-column (Acclaim PepMap 100; 100 µm × 2 cm; nanoViper 2PK; C18; 5 µm; 100 Å) at a flow rate of 300 nl min^{-1}. After desalting, peptides were separated on an analytical column (Acclaim PepMap RSLC; 50 µm × 15 cm; nanoViper; C18; 2 µm; 100 Å) using a linear gradient protocol: 3–8% solvent B over 3 min, 8–28% solvent B over 36 min, 28–45% solvent B over 10 min, 45–90% solvent B over 1 min and 90% solvent B held constant for 10 min. Here, solvent A was 0.1% formic acid and solvent B was 80% acetonitrile with 0.1% formic acid.

The Q Exactive Plus mass spectrometer was run in positive ion mode with a nanospray voltage of 1.8 kV and a source temperature of 275 °C. Mass spectrometry data were collected via automatic switching between MS1 scans and up to 20 tandem mass spectrometry (MS/MS) scans (topN). For MS1 scanning, the target value was set to 1×10^6 within the *m/z* range of 350–2,000, alongside a maximum ion injection time of 50 ms and a resolution of 70,000. Precursor ions were isolated using a window width of 1.6 *m/z*, and the MS/MS fixed initial mass was set to *m/z* 110. Precursor ions were fragmented via high-energy collision dissociation, with a normalized collision energy of 27%. MS/MS scans were acquired at a resolution of 17,500, with a target ion value of 1×10^5 and a maximum ion injection time of 50 ms.

Database search. The *AMELX* gene (*Homo sapiens*; gene ID: 265) encodes three amelogenin isoforms generated through alternative splicing, with UniProt IDs Q99217-1, Q99217-2 and Q99217-3. Among these, Q99217-1 is recognized as the canonical amino acid sequence. Q99217-2 differs from the canonical sequence by lacking amino acid residues 19–34, whereas Q99217-3 contains an insertion of the sequence ENSHAQAINVDRTAL, which replaces the Glu34 residue. Similarly, the *AMELY* gene (*Homo sapiens*; gene ID: 266) produces two protein isoforms (UniProt IDs Q99218-1 and Q99218-2) via alternative splicing. Q99218-2 serves as the canonical amino acid sequence for AMELY. Q99218-1 differs from this canonical sequence by deleting amino acid residues 19–34. Notably, amelogenin isoforms Q99217-3 and Q99218-2 exhibit the greatest degree of similarity.

MS/MS data were processed using MaxQuant software (version 1.6.0.1). Database searches were performed with unspecific digestion settings. The oxidation of methionine (M) and deamidation of asparagine or glutamine (N and Q, respectively) were designated as variable modifications. The minimum peptide length was set to six amino acids. The precursor mass tolerance was adjusted to 10 ppm, whereas the fragment mass tolerance was set to 0.05 Da. The false discovery rate for peptide spectrum matches was set to 0.01. Protein identifications were validated only if they were supported by at least two unique peptide sequences.

The deamidation percentages of glutamine (N) and asparagine (Q) in this study exceeded 90% (Supplementary Table 2) and were significantly higher than the percentages of contaminants (N = 19.52% and Q = 26.49%). Furthermore, no amelogenin-related peptides were found in the blank control group, confirming the reliability of the amelogenin peptide identification.

Isotopic analysis

Strontium, oxygen and carbon isotope analysis of dental enamel. Dental enamel from 49 teeth of 31 individuals at the Songzhuang site was analysed for strontium, oxygen and carbon isotopes. We collected one pig, one dog and nine modern plant samples as references with which to determine the bioavailable $^{87}Sr/^{86}Sr$ around Songzhuang's local area.

Sample pre-treatment varied depending on the material being analysed. For enamel samples, approximately 20 mg of the sample was cut from the tooth, and any adhering dentine or visible dirt contamination were removed. Plant samples were dried and ashed in a muffle furnace at 875 °C, dissolved in hydrofluoric and nitric acid and evaporated to dryness under laminar flow conditions. Salt and lake water were dissolved in ultrapure water and centrifuged, then the supernatant was evaporated to dryness in acid-cleaned Teflon beakers under a laminar flow hood. Following Sr separation routines, all samples were dissolved in ultrapure nitric acid in Teflon beakers on a hot plate at 120 °C overnight. Strontium was purified using cation exchange chromatography with Eichrom's Sr-specific resin (mesh: 100–150 µm; SR-B50-A; Triskem International) and nitric acid as the mobile phase. $^{87}Sr/^{86}Sr$ ratios were measured on an MC-ICP-MS (Neptune Plus) at the CAS Key Laboratory of Crust-Mantle Materials and Environments, School of Earth and Space Sciences, University of Science and Technology of China. The Sr carbonate standard NBS 987 yielded a value of $^{87}Sr/^{86}Sr = 0.710248 \pm 0.000012$ (2 s.d.; $n = 100$).

For carbon and oxygen isotope measurements, enamel samples were prepared in the Archaeometry Laboratory at the University of Science and Technology of China and then sent to the Isotope Laboratory of the Third Institute of Oceanography of the State Oceanic Administration for analysis. Powdered samples were reacted with dehydrated phosphoric acid under vacuum at 70 °C in the headspace of the vial. The $\delta^{18}O$ and $\delta^{13}C$ values of tooth enamel carbonate were then measured using an automated carbonate preparation device (GasBench II) coupled to a gas-ratio mass spectrometer (Delta V; Thermo Fisher Scientific). The isotope ratio measurement was calibrated based on repeated measurements of IAEA-CO-1 and IAEA-CO-8, and the precisions were ±0.2‰ for $\delta^{13}C$ and ±0.2‰ for $\delta^{18}O$ (1 s.d.).

Nitrogen and carbon isotope analysis of dentin serial sections. Tooth tissue recorded isotopic information of the young period. Through dentin sequence analysis of RM1, RM2 and RM3, we were able to reconstruct the life history from birth to approximately 22–23 years of age. In this study, isotopic analysis of dentine serial sections was performed on five individuals, including one female noble (M18), two *renxun* (M1X3 and M18X) and two *rensheng* (M1X5 and M5X4).

Dental samples were prepared for stable isotope analysis following published protocols. Enamel was removed using a dental drill, and the tooth surfaces were cleaned to remove any adhering dirt, cementum

and secondary and/or tertiary dentin, if present. Teeth were demineralized in a 0.5-M HCl solution (CD433036; Codow) at 4 °C for 1–2 weeks, with the HCl solution changed every 24 h. The remains were washed with deionized water to neutrality and rinsed in 0.125 mol l^{-1} NaOH (10011218; SCR) at 4 °C for 20 h, then washed again with deionized water. Serial samples of demineralized dentin were cut at 1-mm intervals transversely. Dentin serial samples were rinsed in 0.001 mol l^{-1} HCl (pH = 3) then gelatinized at 70 °C for 2 days. The heated solution was filtered into the tube and frozen, then freeze-dried for 48 h.

Collagen samples were measured at the isotope-ratio mass spectrometry laboratory of the Third Institute of Oceanography of the State Oceanic Administration using a DELTA V Advantage isotope-ratio mass spectrometer equipped with a Vario EL Ⅲ Element Analyzer (Elementar). Stable isotope concentrations were measured based on international standards (that is, VPDB for carbon and AIR for nitrogen). The analytical precision of the instrument was 0.2‰ for both $\delta^{13}C$ and $\delta^{15}N$.

All collagen samples were well preserved, with an atomic C-to-N ratio between 2.9 and 3.6, a nitrogen concentration above 4.8% and a carbon concentration above 13%, suggesting that these samples could be used for further analysis.

Ancient DNA analysis

Ancient DNA extraction and library preparation. We extracted DNA from 24 samples in a dedicated ancient DNA facility at Fudan University, following established precautions for working with ancient human DNA[106,107]. Human remains were first subjected to surface cleaning and then pulverized into a fine powder. Next, 50 mg of the resulting bone powder was used for DNA extraction[108]. For lysis, 1 ml extraction buffer was dispensed into each 50-mg sample; this buffer comprised 0.45 M EDTA (pH 8.0; AM9262; Thermo Fisher Scientific), 0.25 mg ml^{-1} proteinase K (539480; Merck) and 0.05% (vol/vol) Tween 20 (P9416; Sigma–Aldrich). Following vortex-induced suspension of the sample powder, the mixture was incubated at 37 °C overnight (18–24 h). After centrifugation, the lysate supernatant was decanted into a new tube. Subsequently, 17.5 ml magnetic beads (786-915; G-Biosciences) were combined with 2.5 ml binding buffer including 5 M GuHCl (50933; Sigma–Aldrich), 40% (vol/vol) isopropanol (67-63-0; Sigma–Aldrich), 0.12 M sodium acetate (S2889; Sigma–Aldrich) and 0.05% (vol/vol) Tween 20. Next, 500 µl of the supernatant was added to the binding buffer and bead mixture and subsequent extraction was performed using an automated system (Enlighten Biotechnology)[109]. Lastly, 50 µl TET buffer (Qiagen) was employed for DNA elution. Initial double-stranded, double-indexed libraries were constructed following Meyer's protocols[110], with minor modifications[111,112]. For end repair, 25-µl reactions were set up using 20 µl DNA extract. The reaction mixture was incubated at 12 °C for 20 min, followed by a 15-min incubation at 37 °C. Subsequently, purification was performed using the standard MinElute protocol (28006; Qiagen) and the product was eluted in 15 µl TET buffer (Qiagen).

Next, Illumina-specific adaptors were ligated to the end-repaired DNA in 25-µl reaction volumes. The reaction was incubated at 20 °C for 15 min, after which a second MinElute purification step was conducted; the product was then eluted in 20 µl Buffer EB (Qiagen). Finally, the adaptor fill-in reaction was performed in a total volume of 25 µl. The reaction mixture was incubated at 37 °C for 20 min, followed by a 20-min incubation at 80 °C to inactivate the Bst enzyme (M0275S; New England Biolabs). Libraries were amplified via two parallel PCR reactions using Q5 High-Fidelity DNA Polymerase (M0491S; New England Biolabs) and indexing primers (forward: AGATCGGAAGAGCACACGTCTGAACTCCAGTCAC(index)ATCTCGTATGCCGTCTTCTGCTTG; reverse: AGATCGGAAGAGCGTCGTGTAGGGAAAGAGTGT(index)GTGTAGATCTCGGTGGTCGCCGTATCATT).

Single-stranded libraries were additionally constructed using 30 µl purified extract[113,114]. Indexed products were purified using the MinElute PCR Purification Kit (28006; Qiagen) and the purified libraries were quantified with a Qubit 2.0 fluorometer (Thermo Fisher Scientific).

Shotgun libraries were sequenced on an Illumina HiSeq X10 platform at Annoroad using a 150-base-pair (bp) paired-end strategy. Concurrently, select libraries were converted into circular single-stranded libraries compatible with the DNBSEQ-T7 platform and sequenced at GenePlus (China) using 2× 100-bp chemistry[115].

Nuclear SNP capture and sequencing. Double- and single-stranded shotgun libraries were enriched with the Twist Ancient DNA panel (referred to as Twist 1240k; 106658), adhering to the protocol established at the laboratory of D. Reich. Double-stranded libraries were sequenced on an Illumina NovaSeq 6000 platform at Mingma Technologies (China) with a 150-bp paired-end setup. Single-stranded libraries were sequenced on an Element AVITI platform at Mingma Technologies using a 75-bp paired-end configuration.

Quantification and data analysis. *Sequence data processing*. We trimmed the sequencing adaptors and then merged the paired-end reads into a single sequence using AdapterRemoval version 2.3.2 (ref. 116). The merged reads were mapped to the human reference genome (hs37d5) using the aln command in BWA version 0.7.17 (ref. 117) with the parameters -l 1024 and -n 0.01. Due to some samples being sequenced multiple times, we used the merge function in SAMtools version 1.794 to merge the BAM results from the same human sample, thereby obtaining as many SNPs as possible. Subsequently, we removed PCR duplicates using DeDup version 0.12.8 (ref. 118). To minimize the effect of postmortem DNA damage, we clipped eight bases from both ends of each read using the trimBam function in BamUtil version 1.0.15 (ref. 119). Then, we used mpileup, implemented in SAMtools, with the options -q 30 and -Q 30 to obtain high-quality aligned reads. Finally, we called the pseudo-diploid genotypes using pileupCaller software (https://github.com/stschiff/sequenceTools).

Authentication of ancient DNA. To ensure the credibility of the ancient DNA dataset obtained, we checked the authenticity of the ancient DNA using the following methods. We used PMDtools[120] to calculate the deamination patterns (5′ C > T and 3′ G > A misincorporation) of ancient DNA. We estimated mitochondrial DNA contamination rates using contamMix[121] and the nuclear contamination rate for males with ANGSD version 0.941 (ref. 100). We retained samples that passed at least one of the contamination detection methods: comtamMix (<5%) or ANGSD (<3%).

Genetic sexing and uniparental haplogroup assignment. We compared the genome coverage of the X and Y chromosomes with that of the autosomes to determine the sex of each sample[122]. We called the mitochondrial DNA sequences using schmutzi[123] and assigned the mitochondrial haplogroups using HaploGrep2 (ref. 124). We determined Y haplogroups using the Yleaf program[125] and ISOGG version 15.73 (https://isogg.org/tree/index.html).

Kinship detection. First, to better infer the relatedness of each pair of individuals, we included published data from unrelated individuals from the middle reaches of the Yellow River (YR_LBIA) in our analyses. We used pMMRCalculator (https://github.com/TCLamnidis/pMMRCalculator) to calculate the pairwise mismatch rate and computed relatedness coefficients r for each pair: $r = 1 - (2 \times (x - (b/2))/b)$, where x is the mismatch rate of the pair under analysis and b is the mismatch rate expected for two unrelatived samples with a similar genetic background and overlapping SNPs greater than 100,000. We determined the kinship between the samples based on the cutoff of relatedness coefficients r in the ref. 126. Only results with 10,000 or more overlapping SNPs were considered credible[127]. Second, we used READ2 software[128] with default parameters to detect the genetic kinship between ancient samples. If two samples were second or under-second-degree relatives, we retained one sample with high coverage.

Data merging. We merged our data with previously published present-day and ancient Eurasian genomes from the 1240k and Human Origins datasets, curated by Allen Ancient DNA Resource[129], using the mergeit program in EIGENSOFT[130]. The Human Origin dataset, which contained 597,573 SNPs, was used in smartPCA and admixture analyses. The 1240k dataset, containing 1,233,013 SNPs, was used for other analyses.

PCA. We carried out PCA analysis using smartPCA implemented in EIGENSOFT[130] with the parameters lsqproject: YES and numoutlieriter: 0. The principal components were computed from modern population data, with the ancient populations subsequently projected onto the top two components.

Admixture analysis. We used Plink[131] software with the parameters --indep-pairwise 200 25 0.4 to prune for linkage disequilibrium. Then, we carried out ADMIXTURE version 1.3.0 (ref. 132) analysis from $K = 2$ to $K = 9$ to infer the population clustering patterns in an unsupervised mode with the parameters -B 100 --cv -s time.

Clustering of ancient individuals. We performed a more refined clustering analysis using the qpWave tool from ADMIXTOOLS[133] to test for homogeneity of the samples and found that the samples could be divided into two populations. The samples were subjected to the qpWave test one by one, and when the inclusion of a particular sample led to a P value of <0.05, that sample was deemed to be heterogeneous.

f statistics. We computed *f*-statistics using ADMIXTOOLS[133]. We performed qp3Pop to calculate the outgroup f_3 statistics in the form f_3(A, B; Mbuti) with the parameter inbreed: YES. We calculated f_4 statistics in the form f_4(Mbuti, A; B, C) to explore the additional gene flow between A and B/C relative to C/B using qpDstat with the parameter f4 mode: YES.

Admixture modelling. We used the ADMIXTOOLS[133] software programs qpWave and qpAdm with the parameter allsnps: YES on the merged 1240k dataset. The following populations were used as base outgroups: Mbuti.DG, Russia_MA1_HG.SG, Japan_Jomon, Taiwan_Hanben, YR_MN, DevilsCave_N.SG, Nepal_Samdzong_1500BP.SG, BaBanQinCen and GaoHuaHua.

Statistical analysis

To assess and compare the carbon and nitrogen stable isotope values among different groups in Songzhuang Cemetery, the Shapiro–Wilk test was employed to check whether the data followed a normal distribution. For non-normally distributed data, we used the Mann–Whitney *U*-test or Kruskal–Wallis *H*-test to determine statistical significance. In the case of normally distributed data, Student's *t*-test was utilized. All analyses were two tailed. The SPSS and Origin 2020 software packages were used for statistical analysis and to create graphs of the stable isotope results. The significance level was set at 0.05 and Bonferroni correction was applied for multiple comparisons.

Reporting summary

Further information on research design is available in the Nature Portfolio Reporting Summary linked to this article.

Data availability

Sources for all downloaded data are presented in the supplementary materials. The mass spectrometry proteomics data have been deposited to the ProteomeXchange Consortium (https://proteomecentral.proteomexchange.org) via the iProX partner repository[134,135] with the dataset identifier PXD068097. Alignment files (BAM format) are available from the Genome Warehouse of the National Genomics Data Center, Beijing Institute of Genomics (China National Center for Bioinformation), Chinese Academy of Sciences, under accession number HRA010040, which is publicly accessible at https://ngdc.cncb.ac.cn/gsa-human/. Previously published haploid genotype data of ancient individuals in this study were reported in the David Reich Lab Dataverse: https://dataverse.harvard.edu/dataset.xhtml?persistentId=doi:10.7910/DVN/FFIDCW.

References

1. Bogaard, A., Fochesato, M. & Bowles, S. The farming-inequality nexus: new insights from ancient Western Eurasia. *Antiquity* **93**, 1129–1143 (2019).
2. Haynie, H. J. et al. Pathways to social inequality. *Evol. Hum. Sci.* **3**, e35 (2021).
3. Mattison, S. M., Smith, E. A., Shenk, M. K. & Cochrane, E. E. The evolution of inequality. *Evol. Anthropol.* **25**, 184–199 (2016).
4. Heshmati, A. *Inequalities and Their Measurement* IZA Discussion Paper No. 1219 (Institute for the Study of Labor, 2004).
5. Wells, J. C. K. An evolutionary perspective on social inequality and health disparities: insights from the producer–scrounger game. *Evol. Med. Public Health* **11**, 294–308 (2023).
6. Masclans Latorre, A., Bickle, P. & Hamon, C. Sexual inequalities in the Early Neolithic? Exploring relationships between sexes/genders at the Cemetery of Vedrovice using use-wear analysis, diet and mobility. *J. Archaeol. Method Theory* **28**, 232–273 (2021).
7. Dow, G. K. & Reed, C. G. The economics of early inequality. *Phil. Trans. R. Soc. B* **378**, 20220293 (2023).
8. Mattison, S. M. et al. Market integration, income inequality, and kinship system among the Mosuo of China. *Evol. Hum. Sci.* **5**, e4 (2022).
9. Bai, Y. Quantifying patterns in mortuary practices: an application of factor analysis and cluster analysis to data from the Taosi Site, China. *Open Archaeol.* **8**, 1231–1248 (2022).
10. Bogaard, A. et al. The Global Dynamics of Inequality (GINI) project: analysing archaeological housing data. *Antiquity* **98**, e6 (2024).
11. Squitieri, A. & Altaweel, M. Empires and the acceleration of wealth inequality in the pre-Islamic Near East: an archaeological approach. *Archaeol. Athropol. Sci.* **14**, 190 (2022).
12. Ambrose, S. H., Buikstra, J. & Krueger, H. W. Status and gender differences in diet at Mound 72, Cahokia, revealed by isotopic analysis of bone. *J. Anthropol. Archaeol.* **22**, 217–226 (2003).
13. Hu, Y. Thirty-four years of stable isotopic analyses of ancient skeletons in China: an overview, progress and prospects. *Archaeometry* **60**, 144–156 (2018).
14. Lalueza-Fox, C. *Inequality: A Genetic History* (MIT Press, 2022).
15. Reich, D. *Who We Are and How We Got Here* (Oxford Univ. Press, 2018).
16. Žegarac, A. et al. Ancient genomes provide insights into family structure and the heredity of social status in the early Bronze Age of southeastern Europe. *Sci. Rep.* **11**, 10072 (2021).
17. Mittnik, A. et al. Kinship-based social inequality in Bronze Age Europe. *Science* **366**, 731–734 (2019).
18. Goldberg, A., Günther, T., Rosenberg, N. A. & Jakobsson, M. Ancient X chromosomes reveal contrasting sex bias in Neolithic and Bronze Age Eurasian migrations. *Proc. Natl Acad. Sci. USA* **114**, 2657–2662 (2017).
19. Saag, L. et al. Extensive farming in Estonia started through a sex-biased migration from the Steppe. *Curr. Biol.* **27**, 2185–2193. e6 (2017).
20. Olalde, I. et al. The genomic history of the Iberian Peninsula over the past 8000 years. *Science* **363**, 1230–1234 (2019).
21. Ge, J. *The History of China's Population* (Fudan Univ. Press, 2002).
22. Wang, Y. *The History of China's Population* (Jiangsu People's Publishing House, 1995).
23. Zhao, W. & Xie, S. *The History of China's Population* (People's Publishing House, 1988).

24. Hsu, C.-Y. *Ancient China in Transition: An Analysis of Social Mobility, 722–222 BC* (Stanford Univ. Press, 1966).
25. Li, X. *Eastern Zhou and Qin Civilizations* (Yale Univ. Press, 1985).
26. Tong, S. *History of Spring and Autumn Period* (Zhong Hua Book Company, 2006).
27. Von Falkenhausen, L. *Chinese Society in the Age of Confucius (1000–250 BC): The Archaeological Evidence* (Shanghai Ancient Books Publishing House, 2017).
28. Yu, W. & Gao, M. Research on the system of using tripod in the Zhou Dynasty. *J. Peking Univ.* **1**, 84–97 (1979).
29. Cannon, A. et al. The historical dimension in mortuary expressions of status and sentiment. *Curr. Anthropol.* **30**, 437–458 (1989).
30. Dong, Y., Lin, L., Zhu, X., Luan, F. & Underhill, A. P. Mortuary ritual and social identities during the late Dawenkou period in China. *Antiquity* **93**, 378–392 (2019).
31. Hodder, I. *Symbolic and Structural Archaeology* (Cambridge Univ. Press, 1982).
32. Chen, S. et al. Dietary evidence of incipient social stratification at the Dawenkou type site, China. *Quat. Int.* **521**, 44–53 (2019).
33. Choy, K., Jung, S., Nehlich, O. & Richards, M. P. Stable isotopic analysis of human skeletons from the Sunhung Mural Tomb, Yeongju, Korea: implication for human diet in the Three Kingdoms Period. *Int. J. Osteoarchaeol.* **25**, 313–321 (2015).
34. Lis, B. Foodways in Early Mycenaean Greece: innovative cooking sets and social hierarchy at Mitrou and other settlements on the Greek mainland. *Am. J. Archaeol.* **121**, 183–217 (2017).
35. Eerkens, J. W., Bartelink, E. J., Bartel, J. & Johnson, P. R. Isotopic insights into dietary life history, social status, and food sharing in American Samoa. *Am. Antiq.* **84**, 336–352 (2019).
36. Tao, D., Zhang, G., Zhou, Y., Chen, Z. & Han, G. Population and society in Guanzhuang settlement during Zhou Dynasty based on bioarchaeological perspective. *Acta Anthrop. Sinica* **40**, 320–327 (2021).
37. Zhang, Q. et al. The intersection of diet, class, and sex during the Eastern Zhou (770–221 BCE): bioarchaeological evidence from the Dahan Cemetery, China. *Archaeol. Anthropol. Sci.* **16**, 78 (2024).
38. Zhou, L. Stable isotope analyses of skeletal remains unearthed from Eastern Zhou noble tombs at Chengyangcheng site and other places. *Huaxia Archaeol.* **5**, 60–65 (2020).
39. Zhou, L., Yang, S., Han, Z., Sun, L. & Garvie-Lok, S. J. Social stratification and human diet in the Eastern Zhou China: an isotopic view from the Central Plains. *Arch. Res. Asia* **20**, 100162 (2019).
40. Zhou, L., Han, Z., Sun, L. & Hu, G. Stable isotope analysis of human remains from the Songzhuang Eastern Zhou Cemetery in Qixian, Henan Province: an investigation on the diet of nobles and human sacrifices. *Acta Anthrop. Sinica* **40**, 63–74 (2019).
41. Dong, Y. et al. Shifting diets and the rise of male-biased inequality on the Central Plains of China during Eastern Zhou. *Proc. Natl Acad. Sci. USA* **114**, 932–937 (2017).
42. Dong, Y., Pechenkina, K. & Fan, W. Bioarchaeological evidences of institutionalized gender inequality during Eastern Zhou. *East Asia Archaeol.* 162–173 (2019).
43. Miller, M. J., Dong, Y., Pechenkina, K., Fan, W. & Halcrow, S. E. Raising girls and boys in early China: stable isotope data reveal sex differences in weaning and childhood diets during the Eastern Zhou era. *Am. J. Phys. Anthropol.* **172**, 567–585 (2020).
44. Beck, J. & Quinn, C. P. Balancing the scales: archaeological approaches to social inequality. *World Archaeol.* **54**, 572–583 (2022).
45. Guo, Y. et al. Preliminary report on the excavation of Tomb M4 at the Songzhuang Eastern-Zhou Cemetery, Qi County, Henan. *Huaxia Archaeol.* **4**, 3–11, 153–158, 169, 152 (2015).
46. Bentley, R. A. Strontium isotopes from the earth to the archaeological skeleton: a review. *J. Archaeol. Method Theory* **13**, 135–187 (2006).
47. White, C. D., Spence, M. W., Stuart-Williams, H. L. Q. & Schwarcz, H. P. Oxygen isotopes and the identification of geographical origins: the Valley of Oaxaca versus the Valley of Mexico. *J. Archaeol. Sci.* **25**, 643–655 (1998).
48. Harrison, R. G. & Katzenberg, M. A. Paleodiet studies using stable carbon isotopes from bone apatite and collagen: examples from Southern Ontario and San Nicolas Island, California. *J. Anthropol. Archaeol.* **22**, 227–244 (2003).
49. Liu, H. et al. Combination of the $^{87}Sr/^{86}Sr$ ratio and light stable isotopic values ($\delta^{13}C$, $\delta^{15}N$ and δD) for identifying the geographical origin of winter wheat in China. *Food Chem.* **212**, 367–373 (2016).
50. Zhao, C., Li, Z. & Yuan, J. Strontium isotope analysis of horse and pig tooth enamel from the Yinxu Site, Anyang, Henan. *South. Cult. Relics* **3**, 77–80, 112 (2015).
51. Fang, S. *Strontium Isotope Analysis of Human Migrations of Jiaojia Site* (Shandong Univ., 2018).
52. Zhang, X. et al. Multi-isotope analysis on the Yangtze alligator osteoderm unearthed from Yellow River Valley during the Longshan Period. *Acta Anthrop. Sinica* **40**, 75–86 (2021).
53. Wang, X. & Tang, Z. The first large-scale bioavailable Sr isotope map of China and its implication for provenance studies. *Earth Sci. Rev.* **210**, 103353 (2020).
54. Wang, X. et al. The circulation of ancient animal resources across the Yellow River Basin: a preliminary Bayesian re-evaluation of Sr isotope data from the Early Neolithic to the Western Zhou Dynasty. *Front. Ecol. Evol.* **9**, 583301 (2021).
55. Han, J. A genealogical study of flexed burials in Ancient China. *Cult. Relics* **1**, 53–60, 51 (2006).
56. Yan, S. et al. Y chromosomes of 40% Chinese descend from three Neolithic super-grandfathers. *PLoS ONE* **9**, e105691 (2014).
57. Xue, F. et al. A spatial analysis of genetic structure of human populations in China reveals distinct difference between maternal and paternal lineages. *Eur. J. Hum. Genet.* **16**, 705–717 (2008).
58. Huang, Z. An overview of new data on human sacrifice and retainer sacrifice in Ancient China. *Archaeology* **12**, 53–61 (1996).
59. Jin, G. A study of the burial system of the Qi State nobility during the Eastern Zhou period. *Guan Zi J.* **3**, 59–63 (1994).
60. The Shantung Provincial Museum. Langjiazhuang Tomb 1: an Eastern Zhou human-sacrifice tomb at Linzi, Shandong. *Acta Archaeol. Sinica* **1**, 73–104, 179–196 (1977).
61. Yin, Q. On the human-sacrifice companion tombs of the Qi State during the Eastern Zhou period. *Guan Zi J.* **4**, 115–119 (2015).
62. Yu, J. et al. Wheat for food security in the bronze age: archaeobotanical evidence from the Xichen Site, Eastern China. *Arch. Res. Asia* **41**, 100585 (2025).
63. Tang, L. et al. Study on the utilization of crops in Zhou Dynasty in the Zhengzhou region: a case from Guanzhuang Site, Xingyang. *Quat. Sci.* **42**, 129–143 (2022).
64. Zhao, Z. & Fang, Y. Identification and analysis of the objects floatation-selected from the soil samples collected to the Wangchenggang site in Dengfeng. *Huaxia Archaeol.* **2**, 78–89, 167–168 (2007).
65. Guo, R. et al. Charred plant remains and subsistence economy at the Shilipu North site, Heze, Shandong, during the pre-Qin period. *Agric. Hist. China* **38**, 15–26 (2019).
66. Gong, W., Fang, H., Guo, J. & Chen, X. The impact of climate change on rice agriculture at the end of the Shang period: results of the plant remains from Daxinzhuang and Liujiazhuang sites, Jinan, Shandong Province. *Quat. Sci.* **39**, 170–182 (2019).
67. Tian, C. & Zhou, L. Historical changes in crop cultivation in Northern China: a perspective based on stable isotope analysis of human bone. *J. Zhengzhou Univ.* **53**, 102–106 (2020).
68. Li, C. *Historical Changes of Wheat Cultivation and Its Spread in the Yellow River Valley from Prehistoric Times to the Han Dynasty* (Northwest Univ., 2014).

69. Ling, X. *Study on Qin People's Diet* (Northwest Univ., 2010).
70. Yin, Q. On the transformation of human sacrifice in Qin tombs of the Eastern Zhou period. *East Asia Archaeol*. 60–71 (2023).
71. Song, A. & Dou, H. Analysis of plant food composition of human sacrifices in Xitou site, Xunyi County, Shaanxi Province during the late Shang and early Zhou periods: evidence from starch grains and phytoliths in dental calculus. *Quat. Sci.* **43**, 242–255 (2023).
72. Wang, C. A preliminary analysis of the evolution of the Qin human-sacrifice system. *Res. Qin Han Dynasties* **1**, 246–256 (2021).
73. Fu, Z., Wang, Y., Xu, L., Chen, L. & Li, Z. Preliminary report on the excavation of the Western Zhou tombs at the southwest sector of Dayuan Village, Xixian New Area, Shaanxi Province. *Cult. Relics South. China* **4**, 33–41 (2020).
74. Sun, Y. *C and N Stable Isotope Analysis of Human and Animal Bones from the Hengshui Cemetery* (Shanxi Univ., 2019).
75. Xue, T. *A Study on the Burial System in the State of Ju* (Henan Univ., 2023).
76. Yin, Q. On the Qi State tombs with human sacrificial victims during the Eastern Zhou period. *Guan Zi J.* **4**, 115–119 (2015).
77. Yin, Q. A comparative study of the tombs of human sacrifice in the Qin and Qi states during the Eastern Zhou period. *East Asia Archaeol*. 316–325 (2012).
78. Yin, Q. A preliminary study of human sacrifice in Chu tombs of the Warring States period. *East Asia Archaeol*. 80–89 (2021).
79. Yin, Q. Cultural factors in the Spring-and-Autumn period human-sacrifice tombs of Southeastern Lu: with a discussion of the relationship between Dongyi and Ying-Qin culture. *Fudan J. Humanit. Soc. Sci.* **62**, 50–60 (2020).
80. Yang, M. *A Study of the Western Zhou Yan State Cemetery at Liulihe* (Hebei Univ., 2020).
81. Yin, Q. On the cultural factors of the human-sacrifice tombs at the Xichuan Xiasi Royal Cemetery of the Chu State. *Cult. Relics South. China* **6**, 181–188 (2019).
82. Yin, Q. On human sacrifice in Chu tombs of the Spring-and-Autumn period. *Archaeol. Three Dynasties* **8**, 535–544 (2018).
83. Yang, M. *A Study of Human Sacrifice in the Chu State* (Southwest Univ., 2010).
84. Li, X. et al. Dietary shift and social hierarchy from the Proto-Shang to Zhou Dynasty in the Central Plains of China. *Environ. Res. Lett.* **15**, 035002 (2020).
85. Zhou, L., Garvie-Lok, S. J., Fan, W. & Chu, X. Human diets during the social transition from territorial states to empire: stable isotope analysis of human and animal remains from 770 BCE to 220 CE on the Central Plains of China. *J. Archaeol. Sci. Rep.* **11**, 211–223 (2017).
86. Sun, Y. *Stable Carbon and Nitrogen Isotope Study of Human Bones from Dahekou Western Zhou Cemetery in Yicheng, Shanxi* (Jilin Univ., 2023).
87. Hou, L. et al. Social hierarchy of the Peng state in the Western Zhou Dynasty: stable isotope analysis of animals and humans from the Hengshui Cemetery, Shanxi, China. *J. Archaeol. Sci. Rep.* **44**, 103522 (2022).
88. Gnecchi-Ruscone, G. A. et al. Network of large pedigrees reveals social practices of Avar communities. *Nature* **629**, 376–383 (2024).
89. Knipper, C. et al. Female exogamy and gene pool diversification at the transition from the Final Neolithic to the Early Bronze Age in central Europe. *Proc. Natl Acad. Sci. USA* **114**, 10083–10088 (2017).
90. Rivollat, M. et al. Ancient DNA gives new insights into a Norman Neolithic monumental cemetery dedicated to male elites. *Proc. Natl Acad. Sci. USA* **119**, e2120786119 (2022).
91. Wu, X. et al. Intermarriage and ancient polity alliances: isotopic evidence of cross-regional female exogamy during the Longshan period (2500–1900 BC). *Antiquity* **98**, 48–65 (2024).
92. *The Book of Songs: A Bilingual Edition* (Foreign Language Teaching and Research Press, 2011).
93. *Zuo's Commentary on the Spring and Autumn Annals* (Southeast Univ. Press, 2017).
94. Zuo, Q. *Guoyu: Discourses of the States* (Zhonghua Book Company, 2022).
95. Zeng, T. et al. Ancient DNA reveals the prehistory of the Uralic and Yeniseian peoples. *Nature* **644**, 122–132 (2025).
96. Cao, H. et al. Performance and inter-comparison tests of the MICADAS at the radiocarbon laboratory of Lanzhou University, China. *Radiocarbon* **65**, 41–50 (2022).
97. Bronk Ramsey, C. Bayesian analysis of radiocarbon dates. *Radiocarbon* **51**, 337–360 (2009).
98. Reimer, P. J. et al. The IntCal20 Northern Hemisphere radiocarbon age calibration curve (0–55 cal kBP). *Radiocarbon* **62**, 725–757 (2020).
99. Stewart, N. A., Gerlach, R. F., Gowland, R. L., Gron, K. J. & Montgomery, J. Sex determination of human remains from peptides in tooth enamel. *Proc. Natl Acad. Sci. USA* **114**, 13649–13654 (2017).
100. Fonovic, M., Leskovar, T. & Stamfelj, I. Determination of sex based on sexually dimorphic amelogenin peptides in human tooth enamel. *Ref. Kriminalistikol. K.* **72**, 2 (2021).
101. Welker, F. Palaeoproteomics for human evolution studies. *Quat. Sci. Rev.* **190**, 137–147 (2018).
102. Cappellini, E. et al. Ancient biomolecules and evolutionary inference. *Annu. Rev. Biochem.* **87**, 1029–1060 (2018).
103. Welker, F. et al. The dental proteome of *Homo antecessor*. *Nature* **580**, 235–238 (2020).
104. Tsutaya, T. et al. A male Denisovan mandible from Pleistocene Taiwan. *Science* **388**, 176–180 (2025).
105. Wang, X. et al. Isotopic and proteomic evidence for communal stability at Pre-Pottery Neolithic Jericho in the Southern Levant. *Sci. Rep.* **13**, 16360 (2023).
106. Knapp, M., Clarke, A. C., Horsburgh, K. A. & Matisoo-Smith, E. A. Setting the stage—building and working in an ancient DNA laboratory. *Ann. Anat.* **194**, 3–6 (2012).
107. Du, P. et al. Genomic dynamics of the lower Yellow River Valley since the Early Neolithic. *Curr. Biol.* **34**, 3996–4006 (2024).
108. Rohland, N., Glocke, I., Aximu-Petri, A. & Meyer, M. Extraction of highly degraded DNA from ancient bones, teeth and sediments for high-throughput sequencing. *Nat. Protoc.* **13**, 2447–2461 (2018).
109. Zhu, K. et al. Cultural and demic co-diffusion of Tubo Empire on Tibetan Plateau. *iScience* **25**, 105636 (2022).
110. Meyer, M. & Kircher, M. Illumina sequencing library preparation for highly multiplexed target capture and sequencing. *Cold Spring Harb. Protoc.* **2010**, pdb.prot5448 (2010).
111. Gamba, C. et al. Genome flux and stasis in a five millennium transect of European prehistory. *Nat. Commun.* **5**, 5257 (2014).
112. Allentoft, M. E. et al. Population genomics of Bronze Age Eurasia. *Nature* **522**, 167–172 (2015).
113. Gansauge, M. T., Aximu-Petri, A., Nagel, S. & Meyer, M. Manual and automated preparation of single-stranded DNA libraries for the sequencing of DNA from ancient biological remains and other sources of highly degraded DNA. *Nat. Protoc.* **15**, 2279–2300 (2020).
114. Gansauge, M. T. et al. Single-stranded DNA library preparation from highly degraded DNA using T4 DNA ligase. *Nucleic Acids Res.* **45**, e79 (2017).
115. Zhu, K. et al. Comparative performance of the MGISEQ-2000 and Illumina X-Ten sequencing platforms for paleogenomics. *Front. Genet.* **12**, 745508 (2021).
116. Schubert, M., Lindgreen, S. & Orlando, L. AdapterRemoval v2: rapid adapter trimming, identification, and read merging. *BMC Res. Notes* **9**, 88 (2016).

117. Li, H. & Durbin, R. Fast and accurate short read alignment with Burrows–Wheeler transform. *Bioinformatics* **25**, 1754–1760 (2009).
118. Peltzer, A. et al. EAGER: efficient ancient genome reconstruction. *Genome Biol.* **17**, 60 (2016).
119. Korneliussen, T. S., Albrechtsen, A. & Nielsen, R. ANGSD: analysis of next generation sequencing data. *BMC Bioinformatics* **15**, 356 (2014).
120. Skoglund, P. et al. Separating endogenous ancient DNA from modern day contamination in a Siberian Neandertal. *Proc. Natl Acad. Sci. USA* **111**, 2229–2234 (2014).
121. Fu, Q. et al. DNA analysis of an early modern human from Tianyuan Cave, China. *Proc. Natl Acad. Sci. USA* **110**, 2223–2227 (2013).
122. Fu, Q. et al. The genetic history of Ice Age Europe. *Nature* **534**, 200–205 (2016).
123. Renaud, G., Slon, V., Duggan, A. T. & Kelso, J. Schmutzi: estimation of contamination and endogenous mitochondrial consensus calling for ancient DNA. *Genome Biol.* **16**, 224 (2015).
124. Weissensteiner, H. et al. HaploGrep 2: mitochondrial haplogroup classification in the era of high-throughput sequencing. *Nucleic Acids Res.* **44**, W58–W63 (2016).
125. Ralf, A., Montiel González, D., Zhong, K. & Kayser, M. Yleaf: software for human Y-chromosomal haplogroup inference from next-generation sequencing data. *Mol. Biol. Evol.* **35**, 1291–1294 (2018).
126. Fowler, C. et al. A high-resolution picture of kinship practices in an Early Neolithic tomb. *Nature* **601**, 584–587 (2022).
127. Aktürk, S. et al. Benchmarking kinship estimation tools for ancient genomes using pedigree simulations. *Mol. Ecol. Resour.* **24**, e13960 (2024).
128. Alaçamli, E. et al. READv2: advanced and user-friendly detection of biological relatedness in archaeogenomics. *Genome Biol.* **25**, 216 (2024).
129. Mallick, S. et al. The Allen Ancient DNA Resource (AADR) a curated compendium of ancient human genomes. *Sci. Data* **11**, 182 (2024).
130. Patterson, N., Price, A. L. & Reich, D. Population structure and eigenanalysis. *PLoS Genet.* **2**, e190 (2006).
131. Chang, C. C. et al. Second-generation PLINK: rising to the challenge of larger and richer datasets. *Gigascience* **4**, 7 (2015).
132. Alexander, D. H., Novembre, J. & Lange, K. Fast model-based estimation of ancestry in unrelated individuals. *Genome Res.* **19**, 1655–1664 (2009).
133. Patterson, N. et al. Ancient admixture in human history. *Genetics* **192**, 1065–1093 (2012).
134. Ma, J. et al. iProX: an integrated proteome resource. *Nucleic Acids Res.* **47**, D1211–D1217 (2018).
135. Chen, T. et al. iProX in 2021: connecting proteomics data sharing with big data. *Nucleic Acids Res.* **50**, D1522–D1527 (2021).

Acknowledgements

We thank H. Cao and J. Guo from the Radiocarbon Laboratory of Lanzhou University for assistance with sample dating. We also appreciate the advice provided by W. Ge and B. Yi from Xiamen University on the pre-treatment of isotopes. This work was funded by the National Key Research and Development Program of the Ministry of Science and Technology; the project 'Comprehensive Study on Core Settlements in the Key Stages of the Early Development of Chinese Civilization (1500 to 1000 BC)', along with its sub-project 'Comprehensive Study on Capital Cities and Settlements of the Late Shang Dynasty in the Yellow River Basin' (2022YFF0903602 to Z.G.); the National Key Research and Development Program of China (2020YFC1521607 and 2022YFF0903605 to S.W.; 2023YFC3303701-02 and 2024YFC3306701 to C.-C.W.); the National Natural Science Foundation of China (T2425014 and 32270667 to C.-C.W.; 32070576 to S.W.); the Lantai Youth Scholar Program (2022LTQN602 to S.W.); the Natural Science Foundation of Fujian Province of China (2023J06013 to C.-C.W.); the Major Project of the National Social Science Fund of China (21&ZD285 to C.-C.W.); the Open Research Fund of the State Key Laboratory of Genetic Engineering at Fudan University (SKLGE-2310 to C.-C.W.); the Open Research Fund of the Forensic Genetics Key Laboratory of the Ministry of Public Security (2023FGKFKT07 to C.-C.W.); the Major Special Project of Philosophy and Social Sciences Research of the Ministry of Education (2022JZDZ023 to S.W.); and the four specialized historical and cultural research projects on different periods in Henan Province (Z.G.). The funders had no role in study design, data collection and analysis, decision to publish or preparation of the manuscript.

Author contributions

A.F., S.W. and C.-C.W. conducted the project and conceived of the idea. B.Z., L.S., Y.Z., P.S., Z.G., Z.H., J.W., P.D., J.X., K.W., X.C., B.W. and G.W. collected the samples and conducted the experiments. B.Z., J.Z., X.Z., K.Z., R.W., X.Y., T.B. and Y.X. analysed the data. B.Z., J.Z., C.-C.W., S.W. and A.F. wrote the paper. All authors revised the paper.

Competing interests

The authors declare no competing interests.

Additional information

Supplementary information The online version contains supplementary material available at https://doi.org/10.1038/s41562-025-02356-6.

Correspondence and requests for materials should be addressed to Zhenlong Gao, Chuan-Chao Wang, Shaoqing Wen or Anchuan Fan.

Peer review information *Nature Human Behaviour* thanks the anonymous reviewers for their contribution to the peer review of this work. Peer reviewer reports are available.

Reprints and permissions information is available at www.nature.com/reprints.

Publisher's note Springer Nature remains neutral with regard to jurisdictional claims in published maps and institutional affiliations.

Springer Nature or its licensor (e.g. a society or other partner) holds exclusive rights to this article under a publishing agreement with the author(s) or other rightsholder(s); author self-archiving of the accepted manuscript version of this article is solely governed by the terms of such publishing agreement and applicable law.

© The Author(s), under exclusive licence to Springer Nature Limited 2025

Baoshuai Zhang[1,2,3,12], Jiajing Zheng[4,12], Lei Sun[5,12], Yuanyuan Zhang[1], Zhenlong Gao[5] ✉, Zhaohui Han[5], Pengfei Sheng[2], Xingxiang Zhang[1], Juan Wang[3], Panxin Du[6], Jianxue Xiong[7], Xin Chang[2], Ke Wang[2], Bangyan Wang[8], Kongyang Zhu[4], Rui Wang[9], Xiaomin Yang[10], Tianyou Bai[4], Yu Xu[4], Gao Wu[11], Chuan-Chao Wang[9] ✉, Shaoqing Wen[2,7] ✉ & Anchuan Fan[1,3] ✉

[1]USTC Archaeometry Laboratory, University of Science and Technology of China, Hefei, China. [2]Department of Cultural Heritage and Museology, Fudan University, Shanghai, People's Republic of China. [3]Department of History of Science and Scientific Archaeology, University of Science and Technology of China, Hefei, China. [4]State Key Laboratory of Cellular Stress Biology, School of Life Sciences, Xiamen University, Xiamen, China. [5]Henan Provincial Institute of Cultural Heritage and Archaeology, Zhengzhou, China. [6]State Key Laboratory of Genetic Engineering, Collaborative Innovation Center for Genetics and Development, School of Life Sciences and Human Phenome Institute, Fudan University, Shanghai, China. [7]Institute of Archaeological Science, Fudan University, Shanghai, China. [8]Human Phenome Institute, Fudan University, Shanghai, China. [9]Ministry of Education Key Laboratory of Contemporary Anthropology, Center for Evolutionary Biology, Department of Anthropology and Human Genetics, School of Life Sciences, Fudan University, Shanghai, China. [10]Fujian Provincial Key Laboratory of Philosophy and Social Sciences in Bioanthropology, Institute of Anthropology, Xiamen University, Xiamen, China. [11]Core Facility Center for Life Sciences, University of Science and Technology of China, Hefei, China. [12]These authors contributed equally: Baoshuai Zhang, Jiajing Zheng, Lei Sun. ✉e-mail: 253466072@qq.com; chuanchaowang@fudan.edu.cn; wenshaoqing@fudan.edu.cn; anchuan@ustc.edu.cn

nature portfolio

Corresponding author(s): Zhenlong Gao,Chuan-Chao Wang, Shaoqing Wen, Anchuan Fan

Last updated by author(s): Sep 9, 2025

Reporting Summary

Nature Portfolio wishes to improve the reproducibility of the work that we publish. This form provides structure for consistency and transparency in reporting. For further information on Nature Portfolio policies, see our Editorial Policies and the Editorial Policy Checklist.

Statistics

For all statistical analyses, confirm that the following items are present in the figure legend, table legend, main text, or Methods section.

n/a	Confirmed
☐	☒ The exact sample size (*n*) for each experimental group/condition, given as a discrete number and unit of measurement
☐	☒ A statement on whether measurements were taken from distinct samples or whether the same sample was measured repeatedly
☐	☒ The statistical test(s) used AND whether they are one- or two-sided *Only common tests should be described solely by name; describe more complex techniques in the Methods section.*
☐	☒ A description of all covariates tested
☐	☒ A description of any assumptions or corrections, such as tests of normality and adjustment for multiple comparisons
☐	☒ A full description of the statistical parameters including central tendency (e.g. means) or other basic estimates (e.g. regression coefficient) AND variation (e.g. standard deviation) or associated estimates of uncertainty (e.g. confidence intervals)
☐	☒ For null hypothesis testing, the test statistic (e.g. *F*, *t*, *r*) with confidence intervals, effect sizes, degrees of freedom and *P* value noted *Give P values as exact values whenever suitable.*
☒	☐ For Bayesian analysis, information on the choice of priors and Markov chain Monte Carlo settings
☐	☒ For hierarchical and complex designs, identification of the appropriate level for tests and full reporting of outcomes
☐	☒ Estimates of effect sizes (e.g. Cohen's *d*, Pearson's *r*), indicating how they were calculated

Our web collection on statistics for biologists contains articles on many of the points above.

Software and code

Policy information about availability of computer code

Data collection	We trimmed sequencing adapters and merged paired-end reads into single sequences using AdapterRemoval v2.3.2. Merged reads were mapped to the human reference genome (hs37d5) using the aln program in BWA v0.7.17 with parameters "-l 1024 -n 0.01". For samples sequenced multiple times, BAM results from the same human sample were merged using the merge program in SAMtools v1.7 to maximize SNP recovery. PCR duplicates were removed with Dedup v0.12.8. Based on ancient DNA damage patterns, eight bases were clipped from both ends of each read using the trimBam function in BamUtil v1.0.15. High-quality aligned reads were obtained via mpileup in SAMtools with options "-q 30 -Q 30", and pseudo-diploid genotypes were called using pileupCaller (https://github.com/stschiff/sequenceTools).
Data analysis	To analyze ancient DNA processing, genetic characterization (sex, haplogroups, kinship), population structure, and stable isotope patterns, we used AdapterRemoval v2.3.2, BWA v0.7.17, SAMtools v1.7, Dedup v0.12.8, BamUtil v1.0.15, pileupCaller, pmdtools, contamMix, ANGSD v0.941, schmutzi, Haplogrep2, Yleaf, pMMRCalculator, READ2, EIGENSOFT, Plink, ADMIXTURE v1.3.0, ADMIXTOOLS, SPSS, and Origin 2020.

For manuscripts utilizing custom algorithms or software that are central to the research but not yet described in published literature, software must be made available to editors and reviewers. We strongly encourage code deposition in a community repository (e.g. GitHub). See the Nature Portfolio guidelines for submitting code & software for further information.

Data

Policy information about availability of data

All manuscripts must include a data availability statement. This statement should provide the following information, where applicable:

- Accession codes, unique identifiers, or web links for publicly available datasets
- A description of any restrictions on data availability
- For clinical datasets or third party data, please ensure that the statement adheres to our policy

Sources for all downloaded data are presented in supplementary material. The mass spectrometry proteomics data have been deposited to the ProteomeXchange Consortium (https://proteomecentral.proteomexchange.org) via the iProX partner repository111,112 with the dataset identifier PXD068097. Alignment files (BAM format) are available at the Genome Warehouse in National Genomics Data Center, Beijing Institute of Genomics (China National Center for Bioinformation), Chinese Academy of Sciences, under accession number PRJCA034914 (will be available upon publication), which is publicly accessible at https://bigd.big.ac.cn/gsa.

Research involving human participants, their data, or biological material

Policy information about studies with human participants or human data. See also policy information about sex, gender (identity/presentation), and sexual orientation and race, ethnicity and racism.

Reporting on sex and gender	We reported the biological sex of these individuals via ancient DNA and ancient proteomics analyses. We performed an analysis of the sex ratio of sacrificial humans, which was based solely on biological sex. No other additional analyses related to sex or gender were conducted, as the study focused on the biological attributes of the ancient sacrificial remains.Gender-related information was not collected in this study, as it centers on the biological profiling of these ancient human remains.
Reporting on race, ethnicity, or other socially relevant groupings	We categorized individuals into nobles, commoners, and sacrificial humans based on their archaeological contexts (including burial locations, funerary objects, etc.). These groupings reflect socially constructed status roles identifiable in the archaeological record of the studied site, and detailed information on these groupings is presented in the main text.
Population characteristics	N/A
Recruitment	N/A
Ethics oversight	N/A

Note that full information on the approval of the study protocol must also be provided in the manuscript.

Field-specific reporting

Please select the one below that is the best fit for your research. If you are not sure, read the appropriate sections before making your selection.

☒ Life sciences ☐ Behavioural & social sciences ☐ Ecological, evolutionary & environmental sciences

For a reference copy of the document with all sections, see nature.com/documents/nr-reporting-summary-flat.pdf

Life sciences study design

All studies must disclose on these points even when the disclosure is negative.

Sample size	The sample size was determined by the quantity and preservation quality of the human remains unearthed from the site;it is not something we can choose a priori
Data exclusions	We established assessment indicators for the preservation conditions of ancient DNA and isotopes based on previous studies (see details in the manuscript), and since the samples were well-preserved, no data were excluded.
Replication	Each aliquot of the extract permits the construction of only a single library, so replication using the same extract is not feasible. For individuals with multiple libraries, we verified in all cases that these libraries came from the same individuals.
Randomization	Randomization was not relevant to the study
Blinding	Blinding was not relevant to our study because our research had to take the archaeological context of the samples into consideration.

Reporting for specific materials, systems and methods

We require information from authors about some types of materials, experimental systems and methods used in many studies. Here, indicate whether each material, system or method listed is relevant to your study. If you are not sure if a list item applies to your research, read the appropriate section before selecting a response.

Materials & experimental systems

n/a	Involved in the study
☒	☐ Antibodies
☒	☐ Eukaryotic cell lines
☐	☒ Palaeontology and archaeology
☒	☐ Animals and other organisms
☒	☐ Clinical data
☒	☐ Dual use research of concern
☒	☐ Plants

Methods

n/a	Involved in the study
☒	☐ ChIP-seq
☒	☐ Flow cytometry
☒	☐ MRI-based neuroimaging

Palaeontology and Archaeology

Specimen provenance	We introduced the background of the site in the main text, and supplementary archaeological information for individual samples is provided in Supplementary Table 2.
Specimen deposition	The bone and tooth parts that remain after analysis for isotopes, ancient DNA, and ancient protein are under the stewardship of the archaeologists and cultural institutions from which they were sampled. At present, they are either already returned to the sample steward (Dr. Lei Sun from Henan Provincial Institute of Cultural Relics and Archaeology) or they are stored on long-term loan at the relevant laboratories where they were analysed. They can be re-examined upon request to the sample steward. Researchers who wish to replicate analyses from this study or gather new data on the materials generated for this study are welcome to make a request for aliquots of the relevant samples or libraries to corresponding author Shaoqing Wen, who will fulfill all reasonable requests.
Dating methods	We obtained accelerator mass spectrometry (AMS) radiocarbon dates for 5 distinct human remains at the AMS radiocarbon dating Laboratory of the Key Laboratory of Western China's Environmental Systems (Ministry of Education) at Lanzhou University. We report conventional radiocarbon ages and standard errors. OxCal v.4.4.4 with the IntCal 20 calibration curve was used to calibrate all radiocarbon dates.

☒ Tick this box to confirm that the raw and calibrated dates are available in the paper or in Supplementary Information.

Ethics oversight	All human skeletal remains analysed in this study were sampled with written permission of Dr. Lei Sun from Henan Provincial Institute of Cultural Relics and Archaeology, who is the steward of these skeletal remains. Researchers who wish to obtain further information about specific individuals should write to the corresponding author and/or Dr. Sun Lei, who provided the archaeological contextualisation for these individuals.

Note that full information on the approval of the study protocol must also be provided in the manuscript.

Plants

Seed stocks	N/A
Novel plant genotypes	N/A
Authentication	N/A